

## **SUPPLEMENTAL MATERIAL**

### **Mechanisms of Sinoatrial Node Dysfunction in Heart Failure with Preserved Ejection Fraction**

**Running title:** *SAN dysfunction in HFpEF*

Thassio Mesquita, PhD<sup>1\*</sup>, Rui Zhang, MD<sup>1\*</sup>, Jae Hyung Cho, MD, PhD<sup>1\*</sup>, Rui Zhang, MD<sup>1</sup>, Yen-Nien Lin, MD, PhD<sup>1</sup>, Lizbeth Sanchez, BS<sup>1</sup>, Joshua Goldhaber, MD<sup>1</sup>, Joseph K. Yu, BS<sup>2</sup>, Jialiu A. Liang, BS<sup>2</sup>, Weixin Liu, BS<sup>1</sup>, Natalia A. Trayanova, PhD<sup>2,3</sup>, Eugenio Cingolani, MD<sup>1</sup>

<sup>1</sup>Smidt Heart Institute, Cedars-Sinai Medical Center, Los Angeles, California, USA.

<sup>2</sup>Department of Biomedical Engineering, Johns Hopkins University, Baltimore, Maryland.

<sup>3</sup>Alliance for Cardiovascular and Diagnostic and treatment Innovation (ADVANCE), Johns Hopkins University, Baltimore, Maryland.

\*These authors equally contributed to this work

#### **Address correspondence to:**

Eugenio Cingolani, MD

Smidt Heart Institute, Cedars-Sinai Medical Center

127 S. San Vicente Blvd., Los Angeles, CA 90048

E-mail: eugenio.cingolani@csmc.edu

## Expanded Methods

### ***Animal Models of HFpEF and HFrEF***

All animal experiments were approved by the Cedars-Sinai Institutional Animal Care and Use Committee. A Dahl salt-sensitive (DSS) rat model of HFpEF was used as previously implemented<sup>17</sup>. Briefly, male 7-week-old DSS rats (Charles River Laboratories, MA) were randomly assigned to a high-salt (HS) diet (8% NaCl, Research Diets) to induce HFpEF. DSS rats fed with a normal-salt diet (0.4% NaCl, Research Diets) served as controls. 2-hit HFpEF mouse model was implemented as described<sup>19</sup>. Male C57BL6 mice (8-week-old, Charles River Laboratories, MA) were used. HFpEF was induced by feeding animals with a high-fat diet (60% kilocalories from fat – lard, Research Diets) and supplied with drinking water containing N<sup>ω</sup>-nitro-L-arginine methyl ester (L-NAME; 0.75 g/L, Sigma-Aldrich, pH 7.4 NaOH). Only male rats and mice were used in the experiments since females are less susceptible to dietary salt<sup>58</sup> or high fat diet and L-NAME<sup>59</sup> treatment. Mice fed with standard chow (Teklad) and water served as control. Feeding was continued ad libitum until rats or mice reached the experimental endpoints.

Male Sprague-Dawley rats (8-week-old, Charles River Laboratories, MA) were randomly assigned to sham operation or permanent left anterior descending artery (LAD) ligation to induce myocardial infarction (MI). Briefly, rats were anesthetized with 5% isoflurane inhalation and maintained with 2% isoflurane. After endotracheal intubation, rats were mechanically ventilated. A thoracotomy was performed at the fourth intercostal space to expose the LAD, which was permanently ligated using a 7-0 silk suture. After the chest was closed, the mouse was extubated and allowed to recover from the anesthesia. The sham group underwent the same surgical procedure without LAD ligation. Echocardiography was performed 9 weeks after the MI induction. Animals with ejection fraction <45% were assigned as HFrEF.

## ***Transthoracic Echocardiography, Dobutamine Stress Echocardiography, and Blood Pressure measurements***

Rats or mice were anesthetized with 5% isoflurane (induction) and maintained with 1-2% isoflurane for transthoracic echocardiography (Vevo 3100, VisualSonics). Systolic function was evaluated by the parasternal short-axis view. Diastolic function was assessed from the apical 4-chamber view by measuring E/A and E/E' ratios. E wave (early filling) and A wave (atrial filling) were measured by pulse-wave Doppler mode between the tips of the mitral valve. E' and A' waves were measured with tissue Doppler mode at the septal corner of the mitral annulus (the junction between the anterior mitral leaflet and ventricular septum). Three separate measurements from each animal were averaged to quantify systolic and diastolic function. In a subset of animals, a 30-gauge needle connected to a polyethylene catheter (PE10; Braintree Scientific) filled with saline was inserted into the tail vein for dobutamine administration. After baseline measurements, dobutamine (20 µg/kg) was slowly infused over 1 min. Measurements were made once the elevated HR reached a steady-state, ~2-6 min after dobutamine administration. Stroke volume (SV) was measured using M-mode short axis recordings (VevoLab 5.6.0, VisualSonics) and determined using the following equation:

$$SV = \left( \frac{7.0}{(2.4 + AEDD) \times (AEDD)^3} \right) - \left( \frac{7.0}{(2.4 + AESD) \times (AESD)^3} \right)$$

Where, AEDD is Average End-Diastolic Diameters and AESD is Average End-Systolic Diameters.

Blood pressure was assessed by a non-invasive tail-cuff system dedicated to rodents (BP-2000 series II, Visitech system). All animals underwent a 15 min acclimation period on a heating pad before blood measurements.

## **Heart Failure (HF) score**

HFpEF phenotyping included a HF score criteria, as described<sup>18</sup>. Animals were continuously monitored and scored as follows: appearance (0: normal; 1: mild distress; 2: severe distress), breathing (0: normal; 1: mild tachypnea; 2: labored breathing), mobility (0: normal; 1: decreased activity; 2: severely diminished), edema (0: normal; 1: mild edema; 2: severe edema), and weight (0: >360 g; 1: < 300 g < 360 g; 2: <300 g).

### **Ambulatory ECG recording and chronotropic reserve**

To assess the circadian oscillation of heart rate (HR) and physiological response to maximal exercise test, an ECG telemetry device (CTA-F40 for rat and ETA-F10 for mouse, Data Sciences International, St. Paul, MN) was surgically implanted into the peritoneal cavity and electrodes were arranged subcutaneously in a lead II configuration (negative electrode: right upper chest; positive electrode: left lower abdomen). Telemetry data were recorded and analyzed using Ponemah software (Data Sciences International). A maximal exercise test was performed using a rodent treadmill (Exer-3/6, Columbus Instruments, Columbus, OH). Standard deviations of heart rate during day and night were used as a measure of heart rate variability (HRV). After acclimation at 6 m/min for 20 min, stepwise increases in average speed (2 m/min) were applied every two minutes during treadmill exercise until the animal became exhausted (spending >10 seconds on shocker). Immediately after archiving maximal physical capacity, animals were immediately transferred to the telemetry receiver to record maximal HR and post-exercise HR recovery time.

### ***In vivo $\beta$ -adrenergic receptor stimulation***

HR was measured in anesthetized rats by 29-gauge subdermal needle electrodes to record surface ECG (lead II). Signals were collected at a sampling rate of 1 kHz (PowerLab

4/35, ADInstruments) and analyzed using LabChart software (7 Pro, ADInstruments). After a 5-min stabilization period,  $\beta$ -adrenergic ( $\beta$ -AR) stimulation was carried out by intravenous administration of isoproterenol (100 ng/kg, Sigma-Aldrich) via the tail vein. Body temperature was continuously maintained at  $37 \pm 1$  °C throughout all experimental procedures with a heating pad.

### ***High-Resolution Voltage Maps and Electrograms in sinoatrial (SAN)/Atrial Tissue***

Intact SAN/Atrial preparation was performed, as described<sup>48</sup>. To analyze voltage changes in SAN/atrial tissue, the entire preparation was loaded by immersing the tissue in Tyrode solution containing (in mmol/L): 140 NaCl, 5.4 KCl, 5 HEPES, 5.5 glucose, 1 MgCl<sub>2</sub>, and 1.8 CaCl<sub>2</sub> (pH adjusted to 7.4 with NaOH), and the voltage-sensitive dye RH237 (10  $\mu$ mol/L; Invitrogen #S1109) for 20 min at  $36 \pm 1$  °C. After the loading step, the tissue was washed in a dye-free Tyrode solution containing blebbistatin (10  $\mu$ mol/L; Sigma-Aldrich, #B0560) for 10 min to avoid motion artifacts. The tissue was imaged by high-speed optical voltage mapping (sampled at 1000 frames/s) on a MiCAM05 Ultima-L CMOS camera (100  $\times$  100-pixel CMOS sensor, 10  $\times$  10 mm) (SciMedia) with filters (excitation 520/35 nm, dichroic 560 nm, emission 715 nm long-pass). After baseline recordings, tissue preparation was exposed to increasing doses of isoproterenol (0.1 and 1  $\mu$ mol/L). Optical mapping recordings (5-10 sec) were taken during normal sinus rhythm under the influence of isoproterenol.  $\beta$ -AR stimulation test was conducted after evaluation of SAN function (SNRT).

Optical mapping data were analyzed using RHYTHM for MATLAB software<sup>60</sup>. Raw optical action potentials (OAPs) were filtered in space (3  $\times$  3), in time (low pass Butterworth filter at 150–200 Hz), and 60 Hz noise was removed. If necessary, fluorescent drift was removed with a first- or second-order fitted curve. Activation time was determined by 50% of

the maximum OAP amplitude and used to reconstruct activation maps. The leading pacemaker site was identified as the location of the earliest activation time within the primary SAN region. Leading pacemaker sites within the same preparation were compared to one another under baseline and isoproterenol stimulation (1  $\mu\text{mol/L}$ ). Electrogram (EGM) of the SAN/atrial tissue was recorded using three electrodes, immersed in the bath in close proximity to reduce electrical impedance.

*Ex vivo* SAN function was also assessed by simultaneous optical mapping recordings under S1 pacing stimulation (100 ms duration interval for 10 sec) delivered at the right atrium. Sinoatrial node recovery time corrected by the cycle length at intrinsic sinus rhythm (cSNRT) was used as an index of SAN function. To avoid excessive photobleaching of the dye, 100 ms was chosen as the rapid pacing cycle length for comparison between groups. In a separated cohort of animals, cSNRT tests were conducted in the absence and presence of adenosine (1  $\mu\text{mol/L}$ ) for 10 min.

### ***Quantitative Reverse Transcriptase Polymerase Chain Reaction***

Total RNA was isolated from the SAN tissue using RNeasy Plus Universal Mini Kit (Qiagen) and cDNA was synthesized with 1  $\mu\text{g}$  of RNA using High Capacity RNA-to-cDNA Kit (Applied Biosystems)<sup>17</sup>. Real-time PCR was performed in duplicate using TaqMan Gene Expression Assay probes with specific primers for target sequences. The following assay probes were used: *adrb1* (Rn00824536\_s1) and *adrb2* (Rn00560650\_s1). The  $2^{-\Delta\Delta C_t}$  relative quantification method, using *Ldha* (Rn00820751\_g1) for normalization. Fold change was calculated with  $2^{-\Delta\Delta C_t}$  compared with the control group. Log scale of fold change was used to compare expression levels.

## **Western blot**

Protein was isolated from individual SAN tissue using Bead Ruptor 12 homogenizer (Omni International) with ice-cold RIPA buffer enriched with halt<sup>tm</sup> protease and phosphatase inhibitor cocktail (Thermo Fisher Scientific, #78442) and 5 mM EDTA. Extracts were then centrifuged at 12,000×*g* for 15 min at 4 °C and the protein content was quantified by BCA Protein Assay (Thermo Fisher Scientific, #23227). Western blot was performed with the NuPAGE system (Thermo Fisher Scientific), as described<sup>48</sup>. 25 µg of proteins were resolved on 4-20% gradient gels, transferred onto a PVDF membrane, blocked at room temperature with 5% BSA solution, and incubated with the following primary antibodies: β1-AR (#ab3442, 1:1000, Abcam), β2-AR (#ab182136, 1:1000, Abcam), GRK2 (#sc13143, 1:900, Santa Cruz Biotechnology), pGRK2<sup>Ser670</sup> (#PA5-77851, 1:1000, Invitrogen), GRK5 (#sc-518005 HRP, 1:1000, Santa Cruz Biotechnology), Hcn4 (#APC-052, 1:1000, Alomone), Cav1.3 (#ab85491, 1:500, Abcam), Cav1.2 (#ab84814, 1:1000, Abcam), and GAPDH (#3683S, 1:3000, Cell signaling). All primary antibodies were incubated overnight with blocking solution at 4°C. A secondary antibody (horseradish peroxidase-conjugated, 1: 5,000) was incubated for 60 minutes at room temperature. Immunoreactivity was detected by enhanced chemiluminescent ECL substrate (Thermo Fisher Scientific) and imaged using a ChemiDoc system (Bio-Rad Laboratories). The loading control was run on the same blot.

## **Fibrosis Quantification**

To quantify the amount of fibrosis, SAN tissue was fixed in 10% neutral-buffered formalin solution for 4 h followed by overnight incubation in 30% sucrose at 4 °C before embedding in OCT (Tissue-Tek). Afterward, 5-µm sections were cut perpendicular to the crista terminalis throughout the pacemaker region (head, center, or tail). Hearts from HFrEF animals

were fixed in 10% neutral-buffered formalin solution overnight and subjected to paraffin embedding. Masson's trichrome staining was performed according to the manufacturer's recommendation (Sigma-Aldrich, #HT15). Each slide was scanned with a Leica SCN400 Slide Scanner. Digital images of whole cross-sections of the sample were saved for analysis. Fractional fibrosis (blue-gray pixels divided by total pixels) was measured using ImageJ software. Average results were expressed as the percentage of fibrosis area per total tissue area.

### ***Intracardiac Electrophysiology***

Programmed electrical stimulation (PES) was performed using a 1.6 French octapolar electrophysiology catheter (Millar Instruments) inserted into the right heart via the jugular vein<sup>48</sup>. Sinoatrial node recovery time (SNRT) was measured after applying a 60-sec atrial pacing train at various cycle lengths (150 to 60 ms, 10 ms decrement). All stimulation pulses were given at 3 V for 2 ms, which enabled continuous capture and drive of cardiac conduction. The SNRT was defined as the interval between the last captured atrial pacing stimulus and the onset of first return sinus beat (P wave). Corrected SNRT (cSNRT) was defined as the SNRT minus the baseline intrinsic cycle length before rapid atrial pacing. The longest cSNRT acquired at various cycle lengths from each group was used as used for analysis.

### **Survival analysis**

Rats were monitored at the vivarium at least 2 times per day by independent laboratory staff. Rats too sick to eat or drink were euthanized by recommendation from laboratory staff per institutional animal welfare policy. Criteria for euthanasia were based on an independent assessment by a veterinarian according to AAALAC guidelines. Common reasons for



protocol-mandated euthanasia were progressive weakness (inability to reach water and chow), severe corporal edema, and continuous seizures (more than 5 min). Sudden death was defined as death occurring within 24 hours of last being reported alive.

### **Next-generation RNA sequencing**

Total RNA was isolated from SAN tissue by RNeasy kit using QIAzol (Qiagen). RNA integrity was analyzed on the 2100 Bioanalyzer (RNA RIN values, Online Table IV) using the Agilent RNA 6000 Nano Kit (Agilent Technologies, Santa Clara, CA) and RNA quantified using the Qubit RNA HS Assay Kit (ThermoFisher Scientific, Waltham, MA). Total RNA-Seq library construction was performed using the Swift Biosciences RNA Library Kit (Swift Biosciences, Ann Arbor, MI), following rRNA depletion using Lexogen RiboCop Depletion Kit Human/Mouse/Rat v2 (Lexogen Inc., Greenland, NH). Final library concentration was measured via the Qubit 1X dsDNA HS Assay kit (ThermoFisher Scientific) and library size was evaluated on the 4200 TapeStation using the Agilent D1000 ScreenTape System (Agilent Technologies). Multiplexed libraries were sequenced on a NovaSeq 6000 (Illumina, San Diego, CA) using 75bp single-end sequencing. On average, about 50 million reads were generated from each sample.

### **Bioinformatics and data analysis**

The reads were first mapped to the latest UCSC transcript set using Bowtie2 version 2.1.0 and the gene expression level was estimated using RSEM v1.2.15. TMM (trimmed mean of M-values) was used to normalize the gene expression. Differentially expressed genes were analyzed using the edgeR software. Genes showing altered expression of  $p < 0.05$  (false discovery rate) with greater than 1.5-fold changes were considered differentially expressed.

The pathway analyses were performed using Ingenuity Pathway Analysis software (Qiagen). Goseq was used to perform the GO enrichment analysis. RNA sequencing data have been deposited in National Center for Biotechnology Information's Gene Expression Omnibus under accession number GSE184120.

### **Single SAN Cell Isolation**

We excised the SAN tissue visually by cutting along the crista terminalis and the interatrial septum in prewarmed ( $36 \pm 1$  °C) Tyrode's solution. The tissue obtained was immersed into a low- $\text{Ca}^{2+}$ -low- $\text{Mg}^{2+}$  solution (in mmol/L): 140 NaCl, 5.4 KCl, 0.5  $\text{MgCl}_2$ , 0.2  $\text{CaCl}_2$ , 1.2  $\text{KH}_2\text{PO}_4$ , 50 taurine, 5.5 glucose, 1 mg/mL BSA, and 5 mM HEPES (pH adjusted to 6.9 with NaOH). Then, rat SAN tissue strips were transferred into a warmed low- $\text{Ca}^{2+}$ -low- $\text{Mg}^{2+}$  solution containing collagenase (type II, 230 U/mL, Worthington Biochemical Corporation, #LS004176) and Protease (type XIV, 0.9 U/mL, Sigma-Aldrich, #P5147) for 12-15 min followed by second digestion with Liberase TM (229 U/mL, Roche, #05401151001) for 12-15 min. Mouse SAN tissue was enzymatically digested using Liberase TM (229 U/mL, Roche, #05401151001) for 12-15 min. To stop the digestion process, the SAN was washed using a modified Kraftbrühe (KB) solution (in mmol/L): 70 L-glutamic acid, 20 KCl, 80 KOH, 10  $\text{KH}_2\text{PO}_4$ , 10 taurine, 1 mg/mL BSA, and 10 HEPES (adjusted to pH 7.4 with KOH). Single cells were obtained from the SAN tissue by gentle mechanical trituration with a fire-polished glass pipette in KB solution for 5 min.

### **Single SAN cell electrophysiology**

Experiments were carried out using standard microelectrode whole-cell patch-clamp techniques with an Axopatch 200B amplifier (Molecular Devices) with a sampling rate of 10-

20 kHz and low-pass filtered at 5 kHz. We prepared micropipette electrodes from borosilicate pipettes (TW150F-3; WPI) using a Sutter P-97 electrode puller. 1.5-3 M $\Omega$  resistance pipettes were used. For  $I_{Ca,L}$  recordings, the micropipette electrode solution was composed of (in mmol/L): 110 CsCl, 30 TEACl, 10 NaCl, 0.5 MgCl<sub>2</sub>, 5 MgATP, 5 creatine phosphate, and 10 HEPES (adjusted to pH 7.2 with KOH). The bath solution contained (in mmol/L): 136 NaCl, 5.4 CsCl, 1 MgCl<sub>2</sub>, 1.8 CaCl<sub>2</sub>, 10 HEPES, 10 glucose, and 0.01 TTX (pH adjusted to 7.4 with CsOH). Single SAN cells were depolarized from -55 to -40 mV for 50 ms to inactivate Na<sup>+</sup> current. Then we evoked Ca<sup>2+</sup> current by applying a family of depolarizing voltage steps from -60 to +60 mV (10 mV stepwise for 300 ms). For  $I_{Ca,T}$  recordings, Na<sup>+</sup>-free external solution was used (in mmol/L): 150 N-Methyl-D-glucamine, 2 4-Aminopyridine, 5.4 CsCl, 1.2 MgCl<sub>2</sub>, 2 CaCl<sub>2</sub>, 10 HEPES, 10 glucose, and 0.01 TTX (pH adjusted to 7.4 with CsOH). Total  $I_{Ca}$  (from a holding potential of -90 mV to test pulses from -70 mV to 50 mV (10 mV stepwise for 400 ms) and  $I_{Ca,L}$  (from a holding potential of -50 mV to test pulses in a 10 mV increment, -70 mV to 50 mV, 400 ms) were measured before and after the application of ISO.  $I_{Ca,T}$  was obtained by subtracting  $I_{Ca,L}$  from total  $I_{Ca}$ .

For  $I_f$  recordings, the micropipette electrode solution was composed of (in mmol/L): 128 K-aspartate, 7 KCl, 5 NaCl, 1 MgCl<sub>2</sub>, 1 CaCl<sub>2</sub>; 10 HEPES, 10 EGTA, 6.6 Na-phosphocreatine, and 4 Mg-ATP (pH adjusted to 7.2 with KOH).  $I_f$  was recorded from single cells superfused with Tyrode solution containing BaCl<sub>2</sub> (1 mM). From a -40 mV holding potential, steady-state current amplitudes were calculated at the end of a 2 s step to -140 mV (10 mV stepwise). Each test potential was followed by a step to -140 mV for 1 s to examine its activation kinetics, and then brought to the holding potential of -40 mV. Diastolic membrane potential was recorded using perforated-patch configuration using an intracellular pipette solution composed of (mM): 130 KCl, 10 NaCl, 5 EGTA, 5 Mg-ATP, 5 phosphocreatine,

10 HEPES (pH adjusted to 7.2 with KOH), and with amphotericin B added to a final concentration of 250  $\mu\text{g/mL}$ . Amphotericin B was prepared fresh daily as a 60 mg/ml stock solution in DMSO, and the amphotericin B-containing pipette solution was made fresh hourly by diluting an aliquot of the stock solution into the intracellular solution and vortexing for at least 1 min. Recordings were obtained from cells superfused with warmed Tyrode solution. Only spontaneously beating cells were analyzed.

For  $I_{\text{NCX}}$  recordings, after a series of five 100 ms conditioning pulses at 1 Hz from  $-60$  to  $0$  mV to stabilize SR Ca load, an inward current was evoked by rapid application (spritze) of caffeine 5 mM. The pipette solution for measuring  $I_{\text{NCX}}$  contained (in mmol/L): 110 CsCl, 30 tetraethylammonium Cl, 10 NaCl, 10 HEPES, 0.5  $\text{MgCl}_2$ , 5 phosphocreatine, 5 Mg-ATP (pH adjusted to 7.2 with CsOH). For  $I_{\text{NCX}}$  measurements the bath was a modified Tyrode's solution containing (in mmol/L): 136 NaCl, 5.4 CsCl, 0.33  $\text{NaH}_2\text{PO}_4$ , 1  $\text{MgCl}_2$ , 10 HEPES, 1.8  $\text{CaCl}_2$ , 10 glucose (pH adjusted to 7.4 with NaOH).

### **Spontaneous $\text{Ca}^{2+}$ transient imaging**

To record spontaneous  $\text{Ca}^{2+}$  transient, we immersed the SAN/atrial tissue in Tyrode solution containing the  $\text{Ca}^{2+}$ -sensitive indicator Cal-520/AM (30  $\mu\text{M}$ ; AAT Bioquest) for 60 min at  $35^\circ\text{C}$ . To maintain proper oxygenation of the tissue, a micro magnet agitated the solution during loading. We chose Cal-520 because its signal-to-noise ratio is much higher than the more commonly used fluo-4, allowing lower doses of the indicator to avoid  $\text{Ca}^{2+}$  buffering. After the loading step, the tissue was washed in a dye-free Tyrode solution containing blebbistatin (10  $\mu\text{mol/L}$ ; Sigma-Aldrich, #B0560) for 10 min to avoid motion artifacts and then washed with Tyrode for an additional 15 min before imaging while also increasing the temperature to  $37^\circ\text{C}$ . Images were recorded using the xyt mode (2D) with a resonant scanning confocal microscope

Leica SP5 (Leica Microsystems). We used 488-nm excitation and >505-nm emission with a 10× objective.

### **Ca<sup>2+</sup> Fluorescence measurements**

We recorded Ca<sup>2+</sup> fluorescence signals during voltage-clamp using a custom-designed photometric epifluorescence detection system. Cells were loaded with the Ca<sup>2+</sup> indicator fluo-4 AM by incubating cells in Tyrode containing fluo-4 AM (5 μM) and Pluronic F-127 (0.02%) for 30 minutes, followed by 3 washes for 5 minutes each. Ca<sup>2+</sup> signals were obtained with an inverted microscope used for patching (Zeiss Microscope Axiovert 100TV) using an excitation LED wavelength at 485 nm, and the emission wavelength at >510 nm. Experiments were carried out using a customized recording chamber and cells were continuously perfused with an extracellular solution.

### **Generation of biophysically-detailed *in silico* HFpEF SAN models**

The findings regarding the membrane clock (MC) and Ca<sup>2+</sup> clock (CC) remodeling in HFpEF obtained here were used to construct a biophysically-detailed human HFpEF SAN model. Simulations with the human HFpEF SAN model were conducted to investigate whether MC and CC remodeling can contribute to CI and identify the contribution of each to a specific CI presentation. Ionic remodeling was integrated into a biophysically-detailed human SAN model<sup>39</sup> (available through the CellML Model Repository: <https://models.cellml.org>) in two steps. First,  $I_f$  and  $I_{CaL}$  conductances were reduced (80% and 34%, respectively) to reflect depressed MC currents observed experimentally here. Next, MC and CC parameters affecting Ca<sup>2+</sup> handling (SERCA, RyR, L-type Ca) were tuned to reflect findings regarding dynamics of HFpEF SAN cells at baseline (i.e., without ISO); SAN cells maintained the same beating rate

(BR) and similar  $\text{Ca}^{2+}$  transient amplitudes compared to control. Because fluorescent  $\text{Ca}^{2+}$  imaging only provided relative changes in  $\text{Ca}^{2+}$  concentration, we imposed the additional constraint that diastolic  $\text{Ca}^{2+}$  concentrations could not be lower than that of the original human SAN model. Parameter tuning was achieved in an automated fashion using the Nelder-Mead simplex optimization algorithm<sup>61</sup> as previously described<sup>39</sup> (cost function details can be found in Online Figure XIII). A collection of HFpEF SAN models ( $n = 69$ ), each with distinct MC and CC parameter values that satisfied this constraint (Online Figure XIV, A and Online Table VII), was assessed. Assessing the model dynamics of the entire collection ensures the robustness of modeling findings; this was imperative given the uniqueness of optimized parameters could not be guaranteed due to model complexity and nonlinearity. To test for CI, each model was exposed to a transient 40-s pulse of 1  $\mu\text{M}$  isoproterenol (ISO); max BR, BR response ( $\tau_{\text{on}}$ ), and BR recovery ( $\tau_{\text{off}}$ ) were quantified (Figure 6A, bottom) and compared against the original human SAN model. Lastly, ionic remodeling of each clock was incorporated individually to determine their contributions to CI.

All SAN models were first run for at least 40-s (simulation time) to achieve the steady-state in the absence of ISO. Maximum steady-state BR, BR response ( $\tau_{\text{on}}$ ), and BR recovery ( $\tau_{\text{off}}$ ) were quantified when models were subjected to a transient, ~40-s pulse of 1  $\mu\text{M}$  ISO. These metrics were used to identify the presence and severity of different CI presentations. Max steady-state BR was determined from the last 10 action potentials of the ISO pulse.  $\tau_{\text{on}}$  and  $\tau_{\text{off}}$  were computed using exponential curves fit to the instantaneous BR data with bisquare weighting of the residuals. The biophysical effects of 1  $\mu\text{M}$  ISO were simulated as described in previous published work<sup>39,62</sup>; parameter values are included in Online Table VIII for completeness. The timing and duration of the ISO pulse were adjusted so that its application

and removal occurred at the maximum diastolic potential; this ensured consistency of  $\tau_{on}$  and  $\tau_{off}$  measurements.

Sensitivity analysis was conducted on the collection of HFpEF SAN models to determine how changes in the parameters involved in MC and CC remodeling related to changes in maximal BR under isoproterenol. For each HFpEF model, 200 randomized perturbations were performed on the tuned parameters using the optimization procedure, as well as the conductances for  $I_f$  ( $g_f$ ) and  $I_{CaL}$  ( $P_{CaL}$ ). For a perturbation, each parameter was randomized in the following way. For parameters that underwent the optimization procedure, randomized values were drawn from a normal distribution (mean = nominal parameter value; standard deviation = 10% of nominal parameter value).  $I_f$  and  $I_{CaL}$  conductances were randomly scaled by drawing a scaling factor from a log-normal distribution (mean = 1.0; standard deviation = 0.1). To compute the sensitivity coefficients for each HFpEF SAN model, parameter values of each perturbed model were normalized and collected in the  $X$  ( $200 \times 7$ ) matrix, while maximum BR under isoproterenol of each perturbed model was computed and collected in the  $Y$  ( $200 \times 1$ ) matrix. Next, the sensitivity coefficient matrix,  $B$  ( $7 \times 1$ ), was computed using the equation,  $B = (X^T X)^{-1} X^T Y$ . The final sensitivity coefficients reported are the average of the sensitivity coefficients computed across all HFpEF SAN models.

All simulations were run in MATLAB with numerical integration performed with *ode15s*. All model generation and simulation code will be made available in a Gitlab repository.

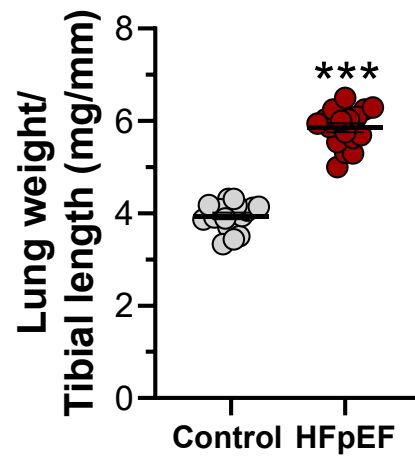
### ***Statistical analysis***

Pooled data are expressed as means  $\pm$  SEM. Statistical comparisons were performed using GraphPad Prism 9 (San Diego, CA, USA). Differences between groups were tested using a two-tailed unpaired Student's t-test, or where repeated measures, either RM-ANOVA

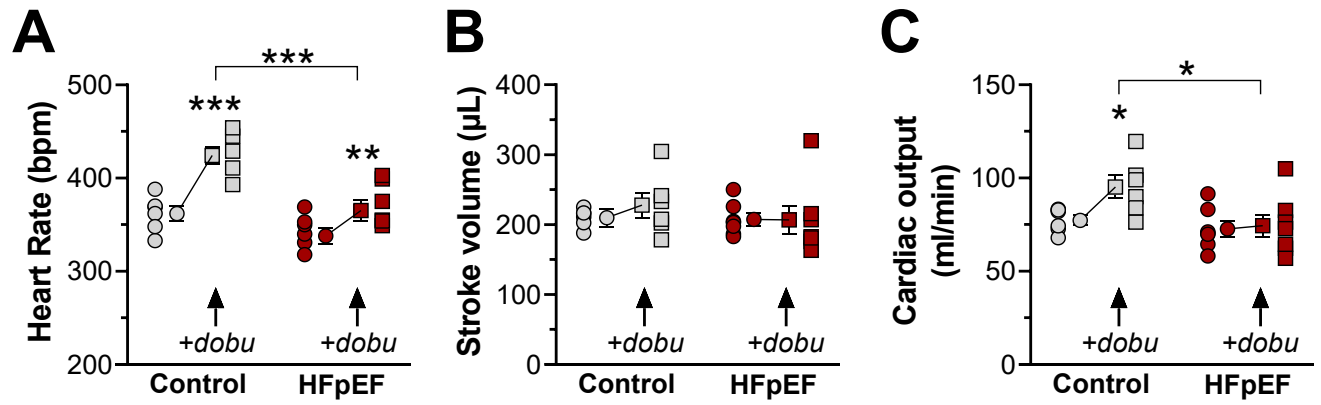
or mixed-effect model when missing data occurred. Post-hoc pairwise testing was Bonferroni corrected for multiple comparisons. Proportions were tested with a Fisher exact test. Kaplan-Meier analysis was used for survival rates with the log-rank test.  $P < 0.05$  was considered statistically significant.



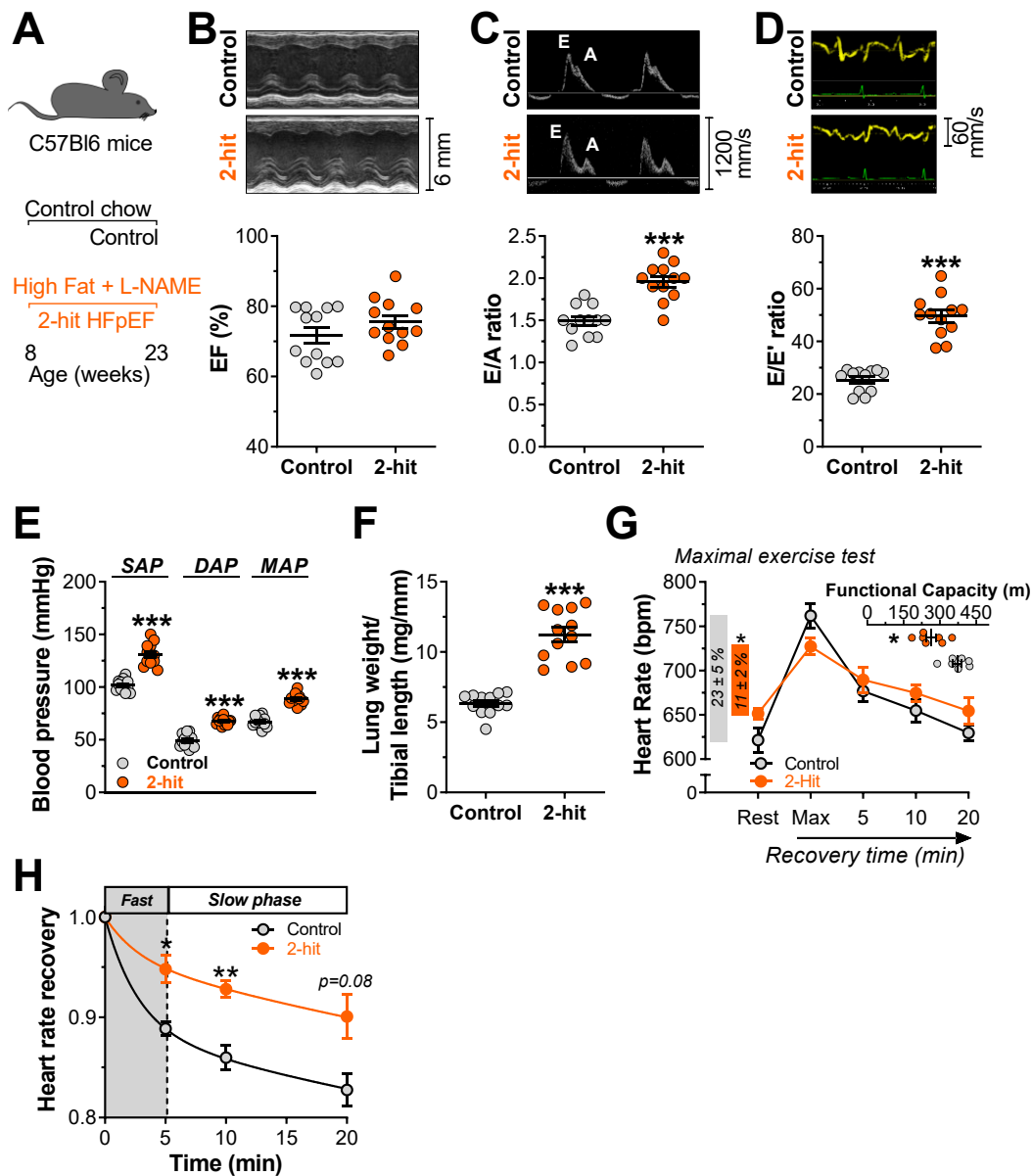
## Online Figures and Legends



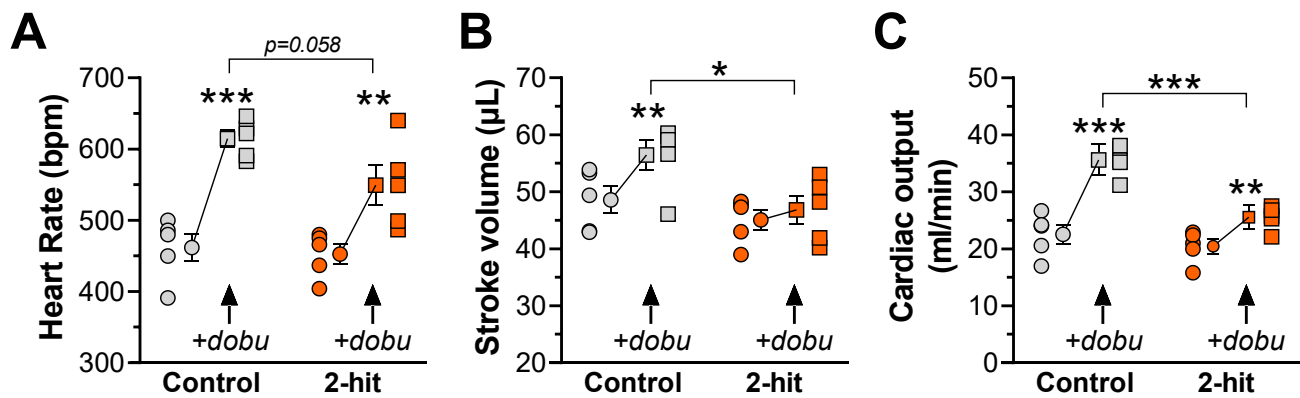
**Online Figure I. Surrogate of pulmonary congestion in HFpEF rats.** Ratio between lung weight and tibia length. Data are expressed as mean  $\pm$  SEM. Unpaired Student's *t*-test. \*\*\* $P < .001$



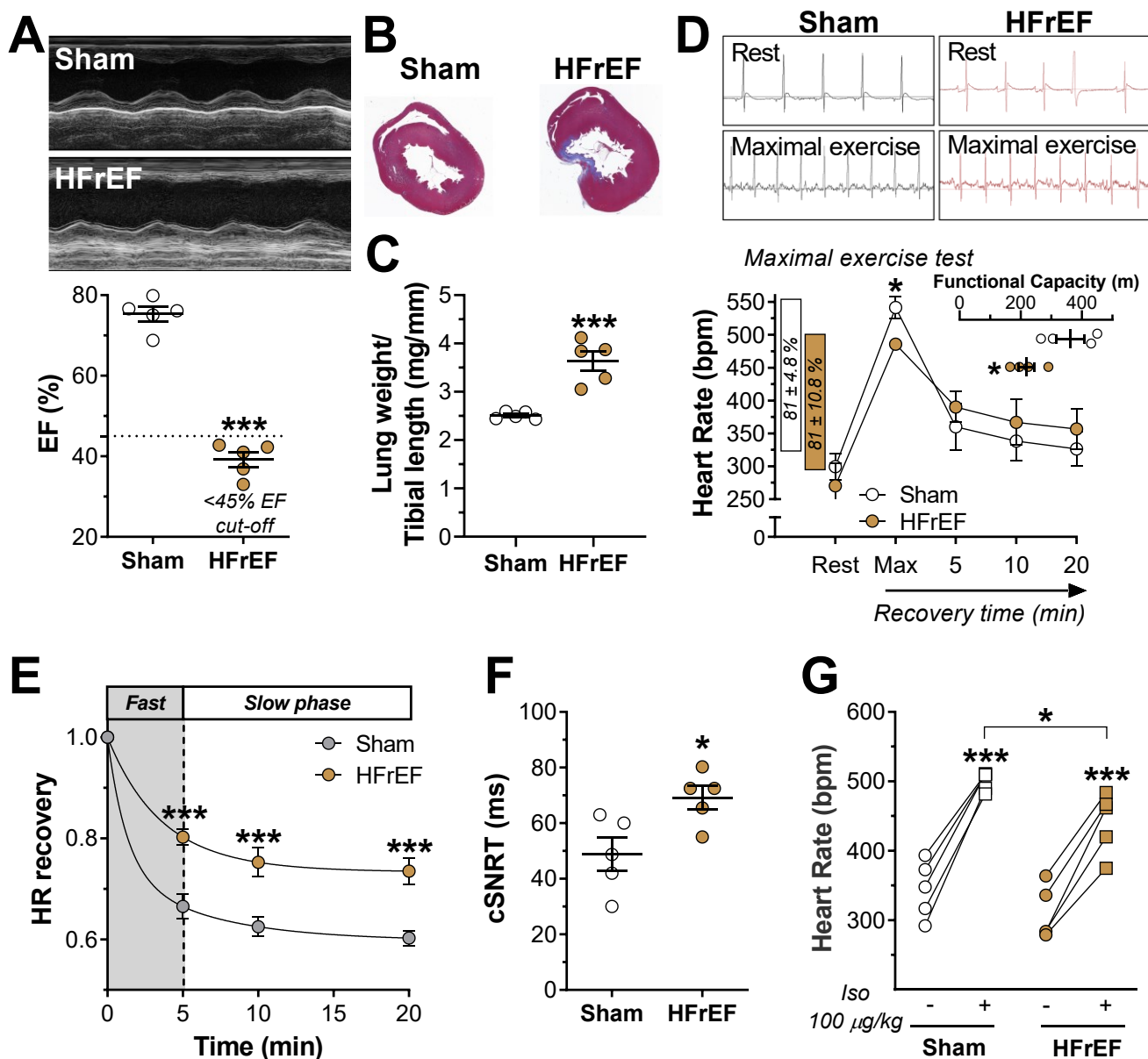
**Online Figure II. Dobutamine stress echocardiography in control and HFpEF rats.** Dobutamine-induced increase in heart rate (A), stroke volume (B), and cardiac output (C) in control and HFpEF animals.  $n = 6$ . Data are expressed as mean  $\pm$  SEM. RM-ANOVA followed by Bonferroni post hoc test. \* $P < .05$ , \*\* $P < .01$ , and \*\*\* $P < .001$ .



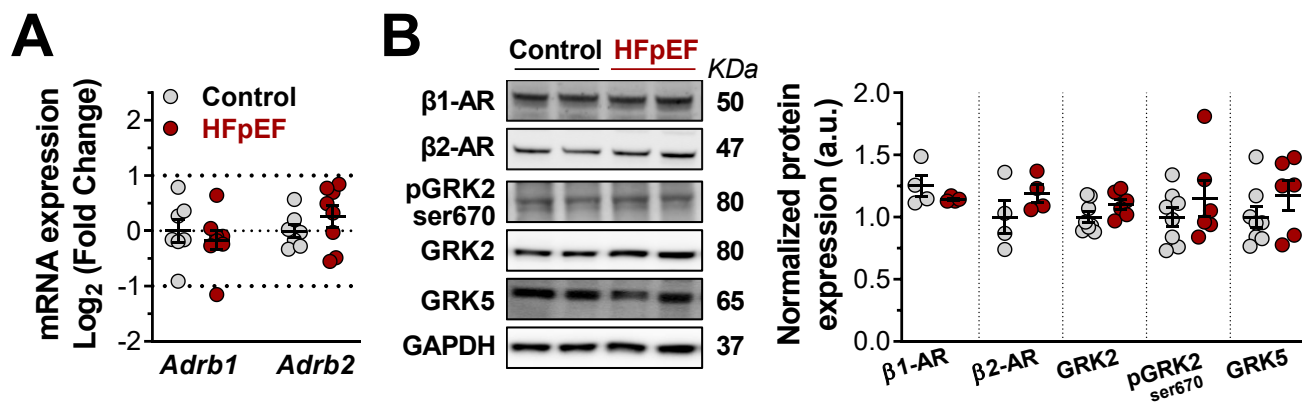
**Online Figure III. A:** Experimental design. Mice were maintained on a standard diet or high-fat diet (60% kilocalories from fat) plus drinking water containing N $\omega$ -nitro-L-arginine methyl ester high salt (L-NAME) dietary regimen from 8 weeks of age and HFpEF verified at 18-23 weeks old. **B:** Representative left ventricular M-mode echocardiographic images (*top*) of ejection fraction (EF) analysis (*bottom*). **C:** Representative images (*top*) of pulse-wave Doppler showing E (early filling)– and A (atrial filling)–wave changes (*bottom*). **D:** Representative images (*top*) of tissue Doppler describing E'– and A'–wave changes (*bottom*). **E:** Noninvasive blood pressure measurements. DAP = diastolic arterial pressure; MAP = mean arterial pressure; SAP = systolic arterial pressure. **F:** Lung weight and tibia length ratio. **G:** Resting, maximal, and recovery of heart rate in response to exercise test (inset, functional capacity measured as the total running distance).  $n = 7$  animals in each group. **H:** Heart rate recovery after the maximal exercise test, data are fit by two exponential decay fit. Data are expressed as mean  $\pm$  SEM. Unpaired Student *t*-test (B–F, G insets). RM-ANOVA followed by Bonferroni post hoc test (G and H). \* $P < .05$ , \*\* $P < .01$ , and \*\*\* $P < .001$ .



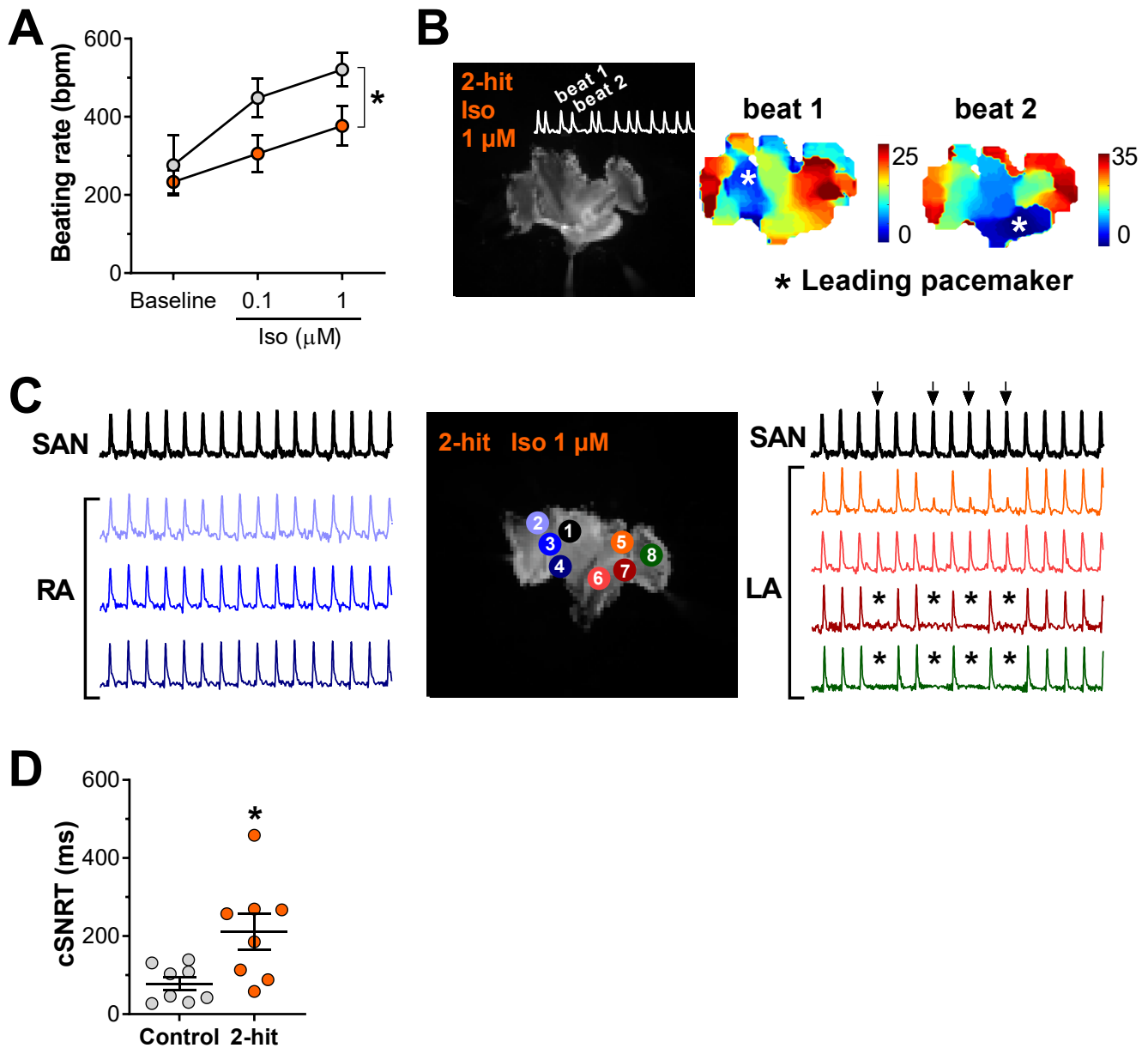
**Online Figure IV. Dobutamine stress echocardiography in control and 2-hit HFpEF mouse.** Dobutamine-induced increase in heart rate (A), stroke volume (B), and cardiac output (C) in control and 2-hit HFpEF animals.  $n = 5$ . Data are expressed as mean  $\pm$  SEM. RM-ANOVA followed by Bonferroni post hoc test. \* $P < .05$ , \*\* $P < .01$ , and \*\*\* $P < .001$ .



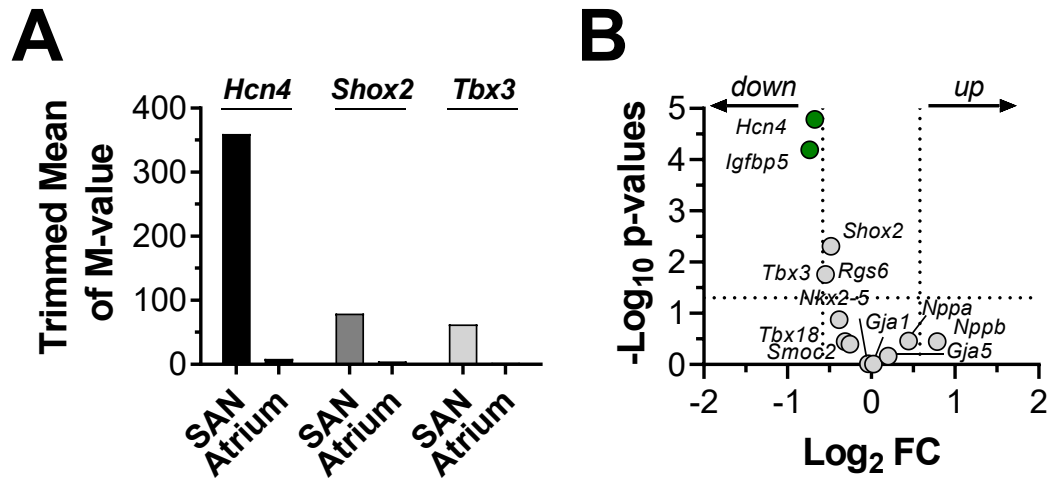
**Online Figure V. Chronotropic response and SAN function in HFrEF.** **A:** Representative left ventricular M-mode echocardiographic images (*top*) of ejection fraction (EF) analysis (*bottom*). **B:** Representative Masson's trichrome-stained sections of ventricular samples **C:** Lung weight and tibia length ratio. **D:** Resting, maximal, and recovery of heart rate in response to exercise test (inset, functional capacity measured as the total running distance).  $n = 4$  animals in each group. **E:** Heart rate recovery after the maximal exercise test, data are fit by two exponential decay. **F:** Quantification of *in vivo* corrected SAN recovery time (cSNRT, corrected by intrinsic CL = cycle length). **G:** Quantification of  $\beta$ -adrenergic-induced heart rate increase (Iso = isoproterenol). Data are expressed as mean  $\pm$  SEM. Unpaired Student *t*-test (A, C, D insets, and F). RM-ANOVA followed by Bonferroni post hoc test (D, E, and G). \* $P < .05$  and \*\*\* $P < .001$ .



**Online Figure VI. Unchanged  $\beta$ -adrenergic receptors and G protein-coupled receptor kinases in HFpEF SAN.** **A:** mRNA expression of  $\beta$ -adrenergic receptors isoforms (*Adrb1* and *Adrb2*). **B:** Representative western blot images (*left*) and quantification protein expression of  $\beta$ -adrenergic receptors and G protein-coupled receptor kinases (GRK) isoforms (*right*). Data are expressed as mean  $\pm$  SEM. Unpaired Student's *t* test.

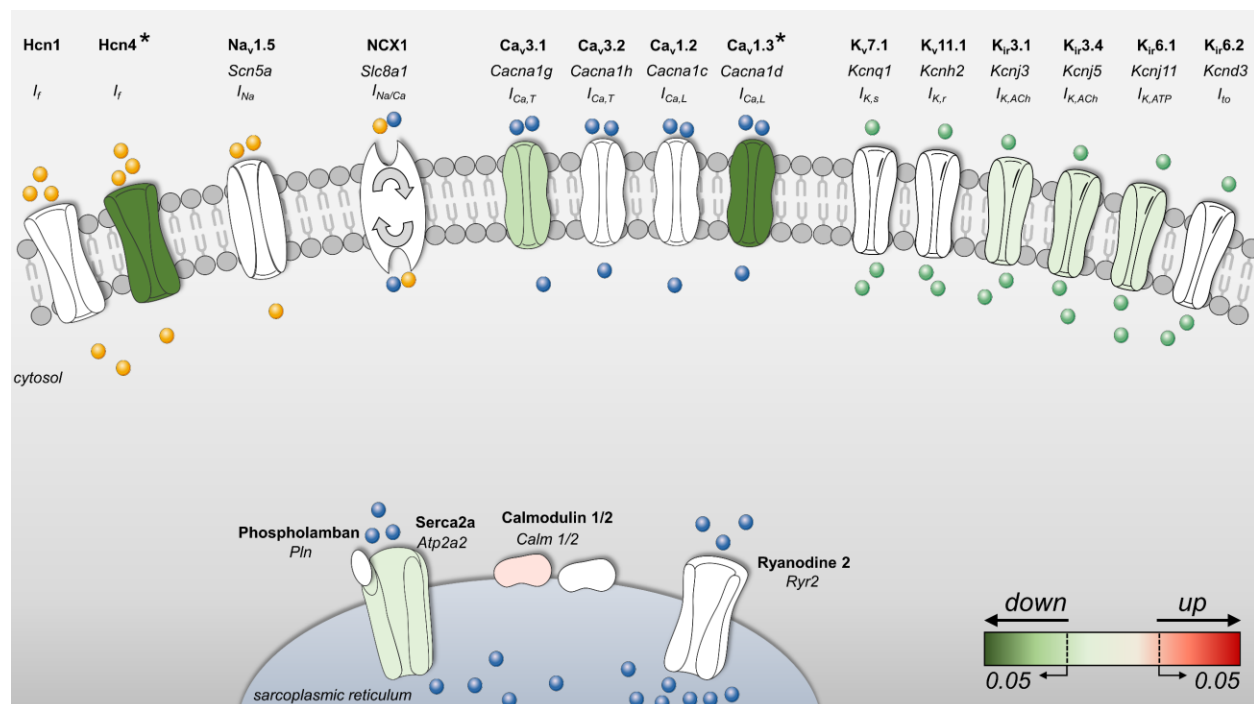


**Online Figure VII. SAN function in phenotypically verified 2-hit HFpEF mice.** **A:** Spontaneous sinus rhythm and concentration-response curve for isoproterenol (Iso) were used to evaluate *ex vivo* beating rate. N = 8 animals in each group. **B:** *left*, Representative *ex vivo* SAN/atrial tissue loaded with a voltage-sensitive dye (inset, representative optical action potential traces), *right*, representative isochronal voltage maps under isoproterenol (Iso) stimulation; \* denotes the location of the SAN leading pacemaker, defined as the earliest activation site. **C:** Overview of HFpEF SAN/atrial preparation; \* denotes the presence of conduction blocks. **D:** Corrected SAN recovery time (cSNRT, corrected by intrinsic CL= cycle length) was measured using *ex vivo* SAN/atrial tissue preparation loaded with a voltage-sensitive dye. Data are expressed as mean  $\pm$  SEM. RM-ANOVA followed by Bonferroni post hoc test (A). Unpaired Student *t*-test (D). \*P < .05.

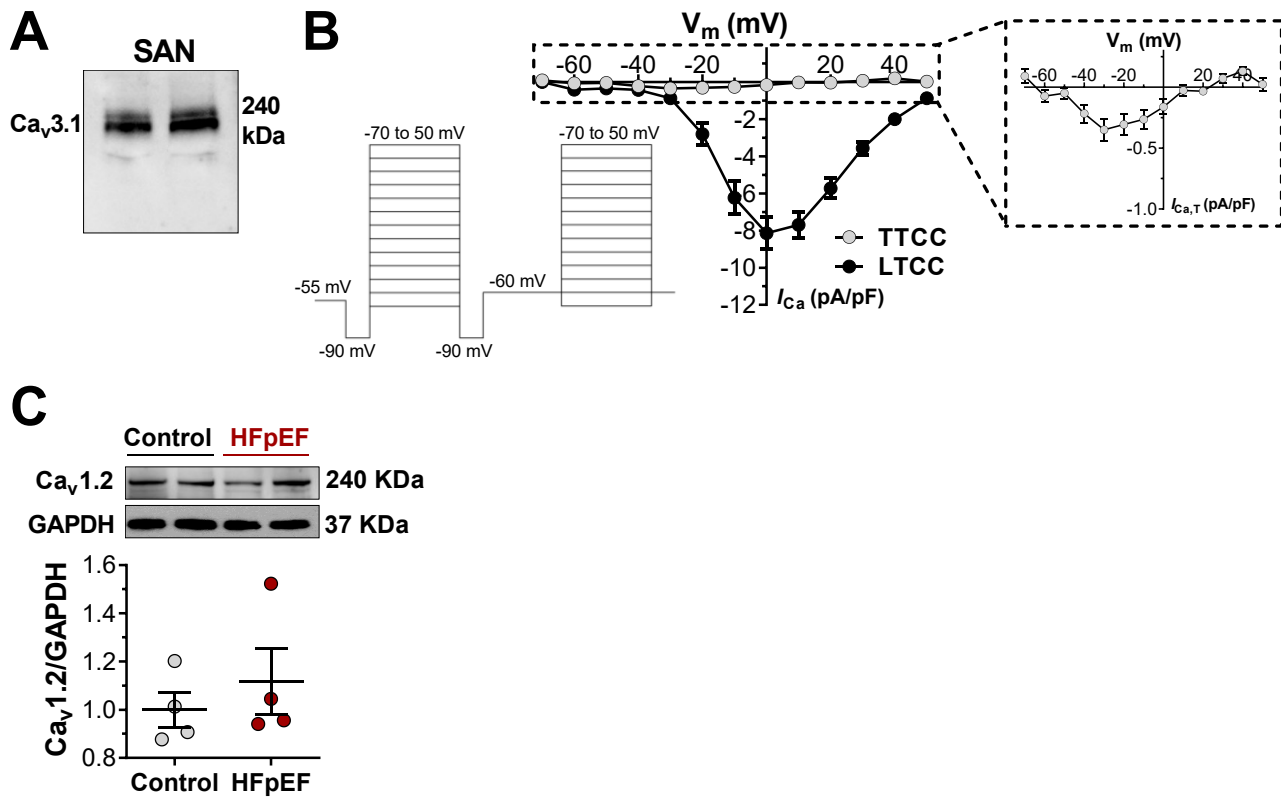


**Online Figure VIII. SAN-specificity RNA sequencing and lack of molecular shift towards a less nodal phenotype in SAN of HFpEF. A:** RNA sequencing revealed a large enrichment of *Hcn4*, *Shox2*, and *Tbx3* gene expression in the SAN tissue compared to atrial tissue. **B:** Volcano plot of fold change relative to control SAN. Highlighted genes are critically related to the differential compact and transitional SAN cell population, as demonstrated<sup>29</sup>.

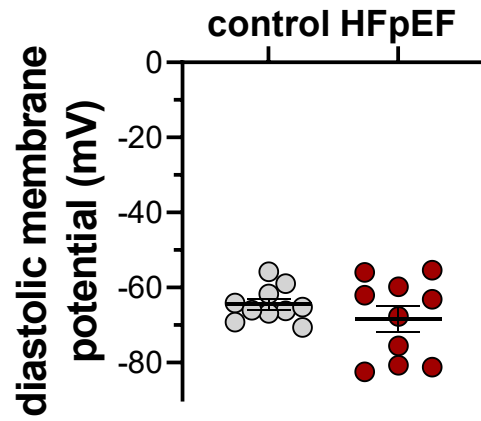




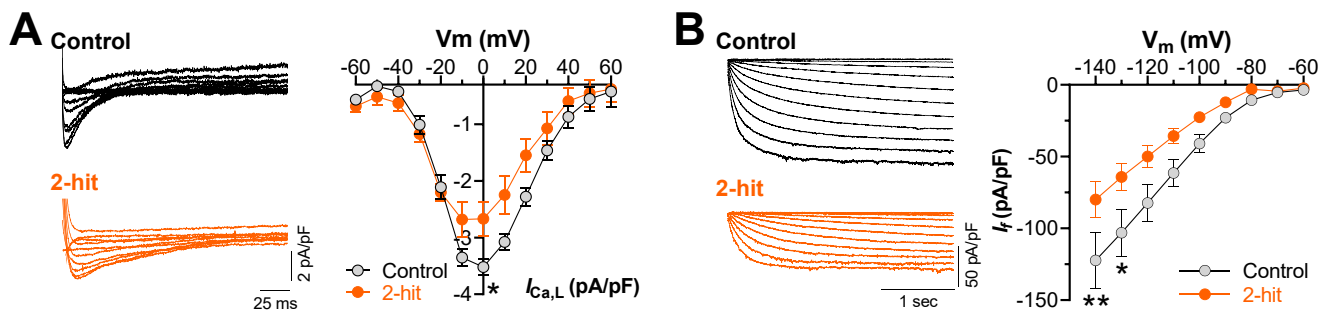
**Online Figure IX. Schematic representation of genes involved in pacemaker generation (Membrane and  $\text{Ca}^{2+}$  clock) in the HFpEF SAN.** Genes are colored by differential expression compared to control SAN. Values are provided in Online Table IV.



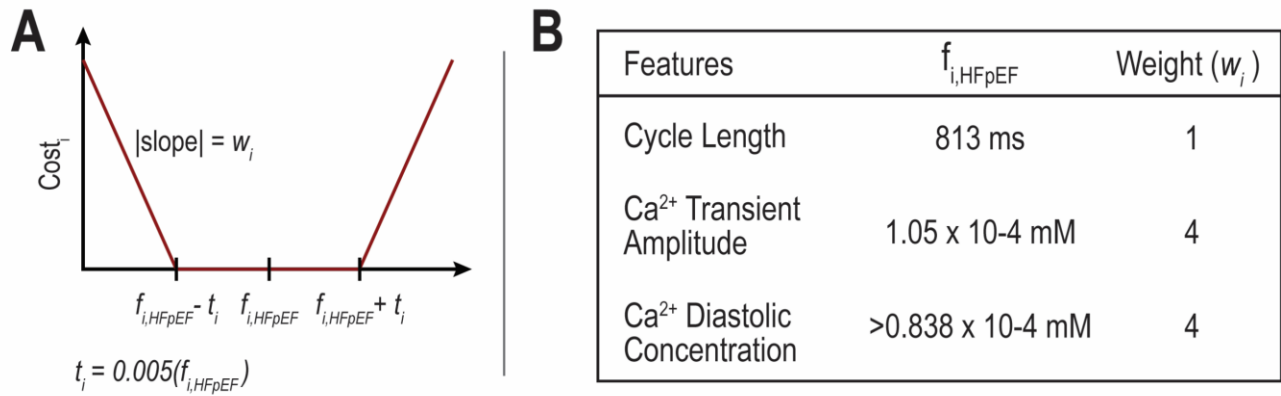
**Online Figure X. Larger functional contribution of L-type Ca<sup>2+</sup> channels in rat SAN cells.**  
**A:** Representative western blot image in control SAN tissue. **B:** L-type and T-type Ca<sup>2+</sup> channels current densities recorded in control isolated SAN cells (n= 12 cells from 4 animals), inset highlights the Ca<sup>2+</sup> currents through T-type Ca<sup>2+</sup> channels. **C:** Representative western blot images (*top*) and quantification of Ca<sub>v</sub>1.2 protein expression (*bottom*). Data are expressed as mean ± SEM. Unpaired Student's *t*-test (C).



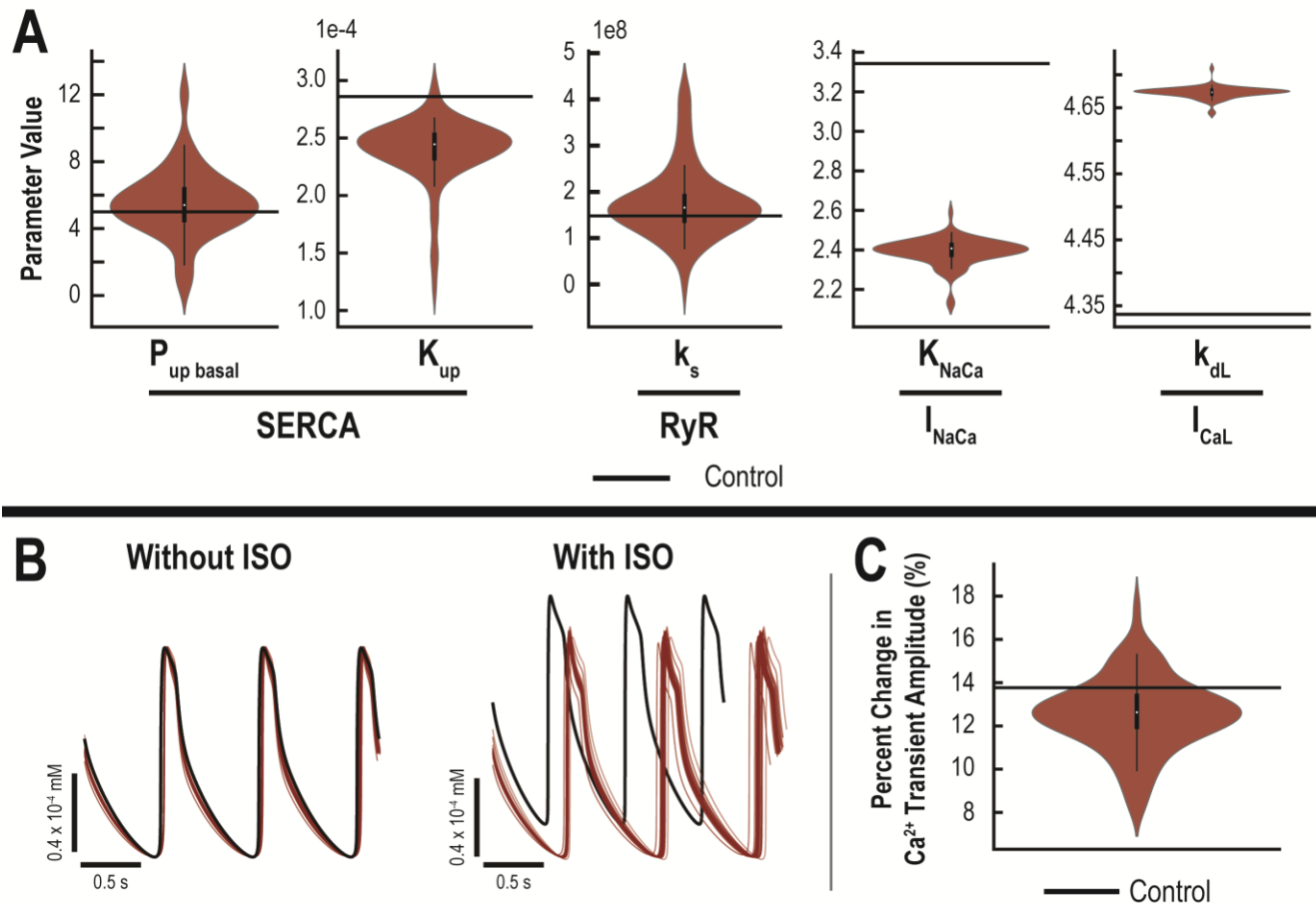
**Online Figure XI. Unchanged maximal diastolic membrane potential in SAN from HFpEF rats.** N = 10 cells from 3 animals. Data are expressed as mean  $\pm$  SEM. Unpaired Student's *t* test.



**Online Figure XII. Modest suppression L-type  $\text{Ca}^{2+}$  and funny current in 2-hit HFpEF mice.** **A:** *left*, Representative L-type  $\text{Ca}^{2+}$  channel currents recorded in isolated mouse SAN cells; *right*, average peak current density–voltage relationship of  $I_{\text{Ca,L}}$  in control (n= 11 cells from 4 animals) and 2-hit HFpEF (n= 9 cells from 4 animals). **B:** Representative funny currents ( $I_f$ ) recorded in isolated mouse SAN cells; *right*, average peak current density-voltage relationship of  $I_f$  in control (n= 12 cells from 3 animals) and 2-hit HFpEF (n= 12 cells from 3 animals). RM-ANOVA followed by Bonferroni post hoc test (A and B). \*P < .05 and \*\*P < .01.

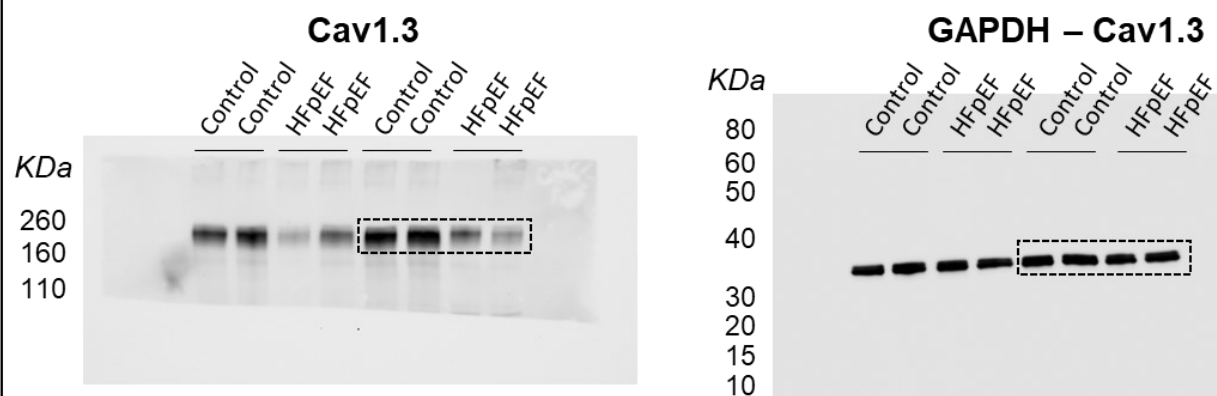


**Online Figure XIII. HFpEF membrane and Ca<sup>2+</sup> clock modeling parameters. A:** Cost function of feature  $i$  to the total cost (i.e., summed over all features). **B:** Nominal feature values ( $f_{i, HFpEF}$ ) and corresponding weights.

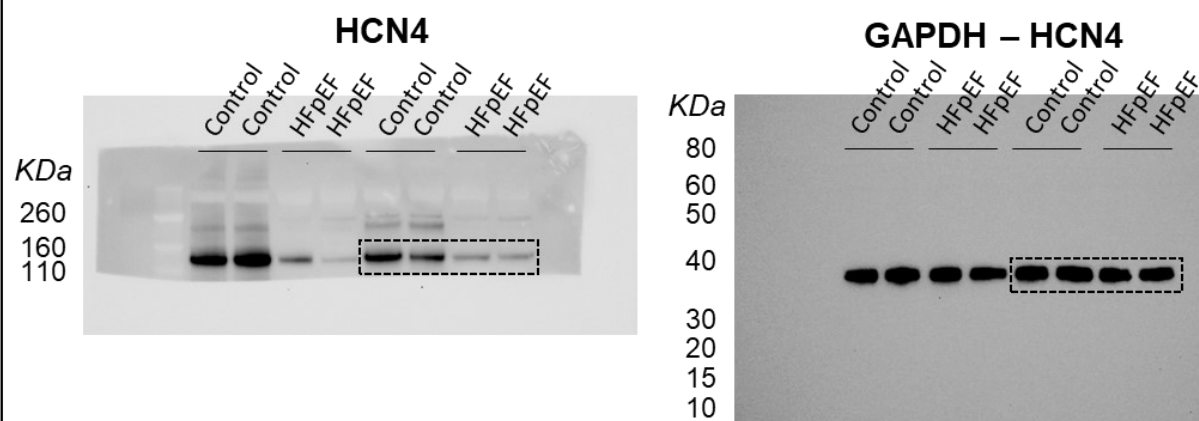


**Online Figure XIV. Additional details and validation of *in silico* HFpEF SAN models.** **A:** Violin plot showing the distribution of optimized  $\text{Ca}^{2+}$  clock parameters of HFpEF SAN models.  $P_{\text{up basal}}$ : Basal rate constant for  $\text{Ca}^{2+}$  uptake by SERCA pump into sarcoplasmic reticulum;  $K_{\text{up}}$ : half-maximal  $\text{Ca}_i$  for  $\text{Ca}^{2+}$  uptake into sarcoplasmic reticulum;  $k_s$ : maximal rate of  $\text{Ca}^{2+}$  release from RyR channels;  $K_{\text{NaCa}}$ : maximal current of NCX;  $k_{\text{dL}}$ : slope factor of L-type voltage-dependent activation gate dL. **B:** Representative steady-state  $\text{Ca}^{2+}$  transient traces of HFpEF models (red) and control (black) without (left) and with (right) isoproterenol (ISO 1  $\mu\text{M}$ ). **C:** % change of  $\text{Ca}^{2+}$  transient amplitude of HFpEF models after ISO stimulation.

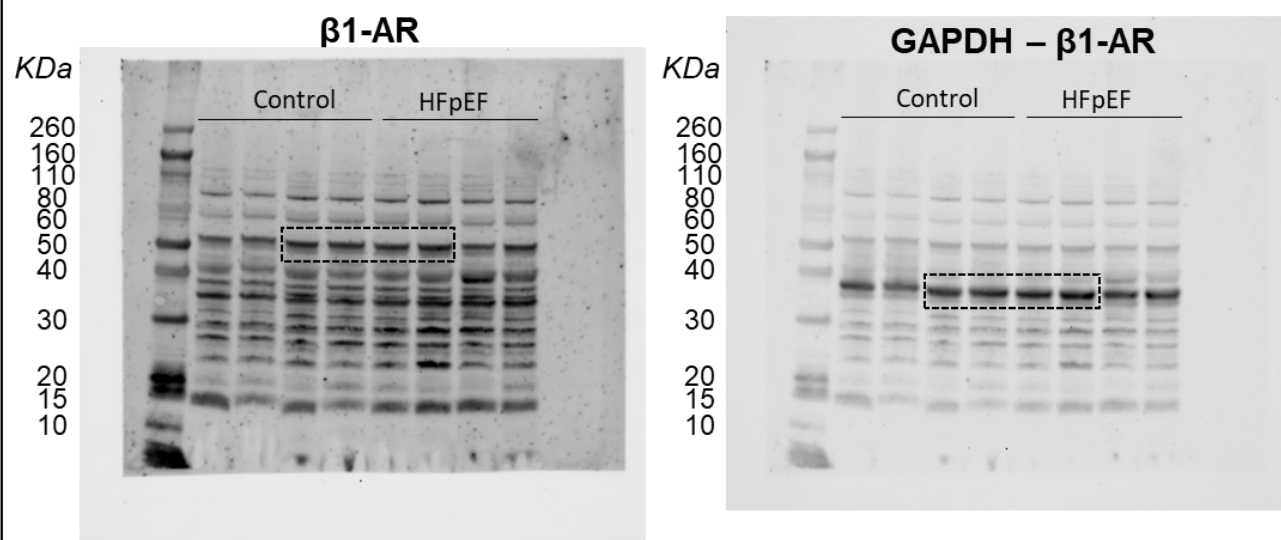
### Full unedited gel for Figure 4C



### Full unedited gel for Figure 4I

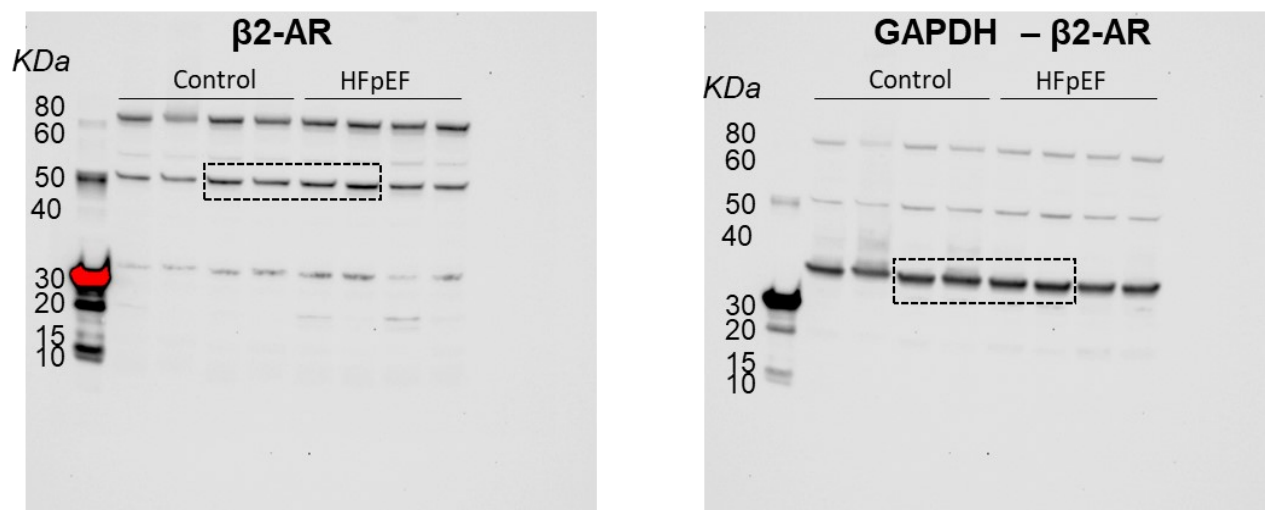


### Full unedited gel for Supplementary Figure 1B

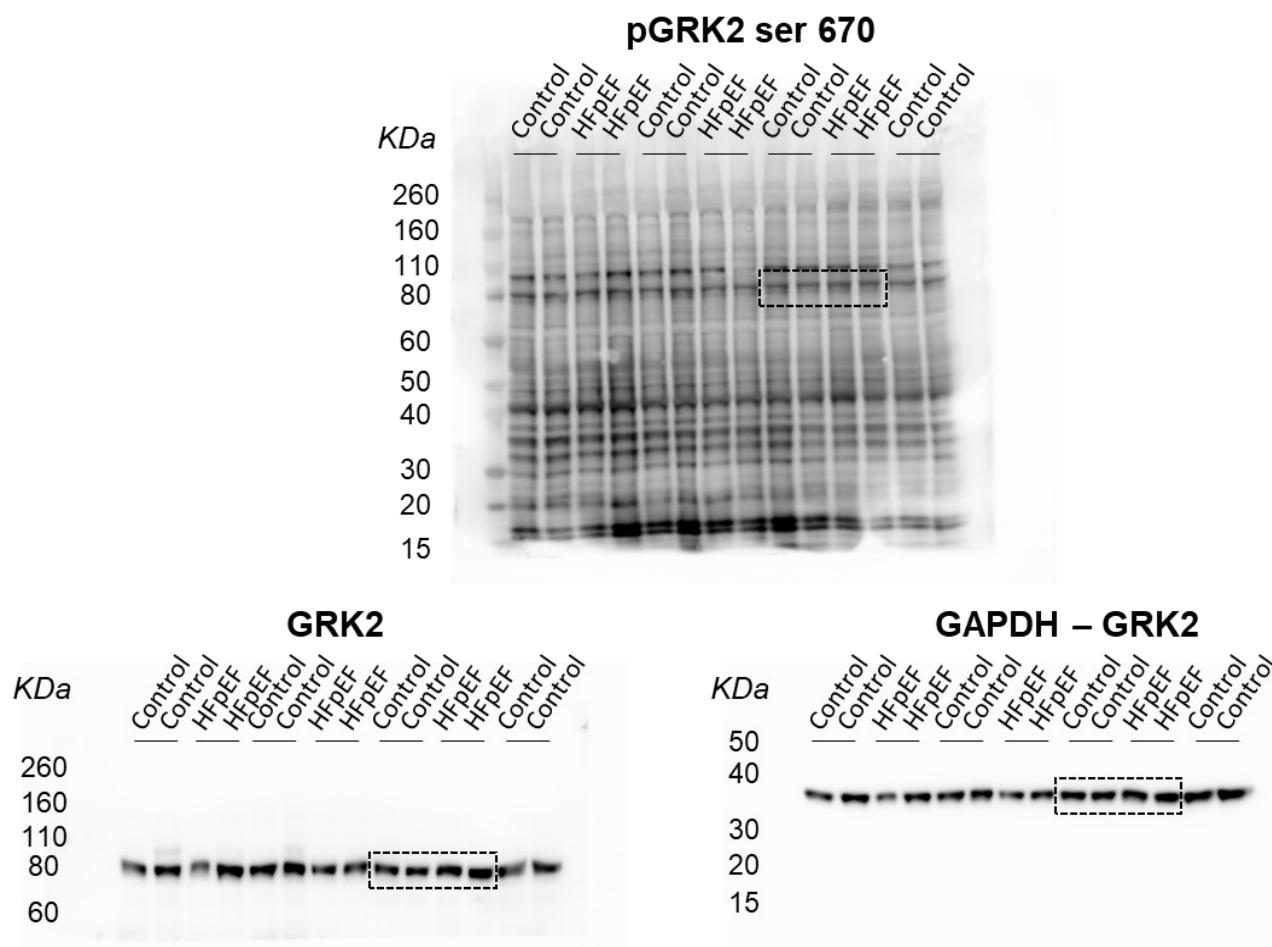


Online Figure XV. Uncut gel blot . (Continued)

## Full unedited gel for Supplementary Figure 1B



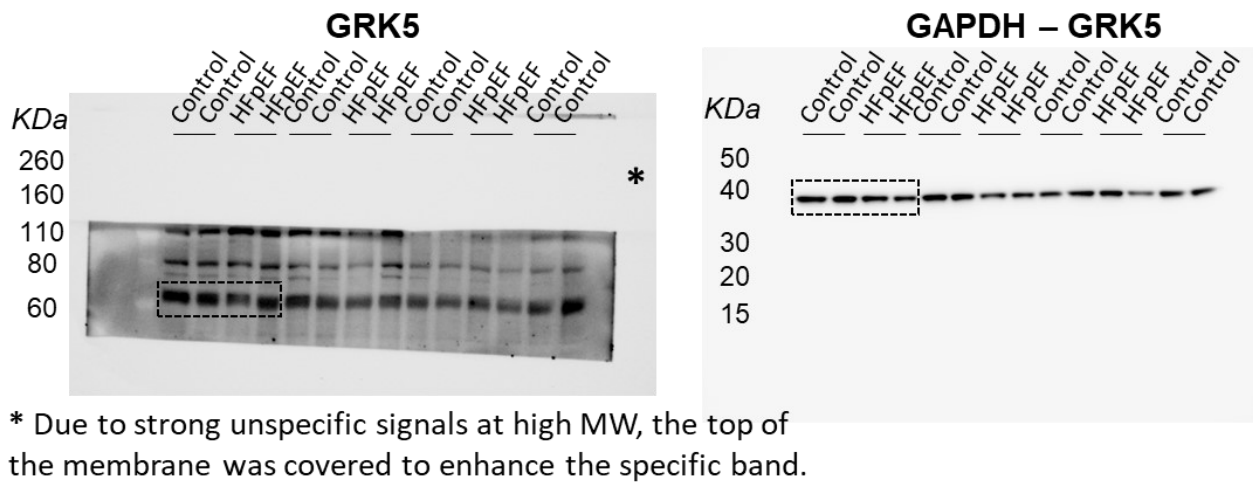
## Full unedited gel for Supplementary Figure 1B



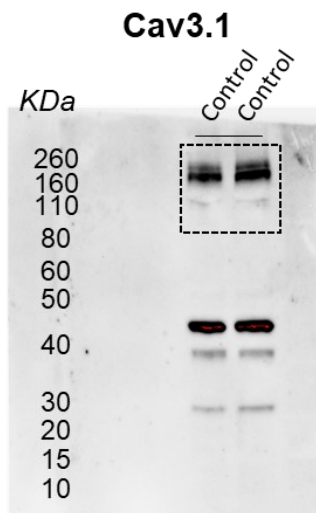
Online Figure XV. Uncut gel blot. (Continued)



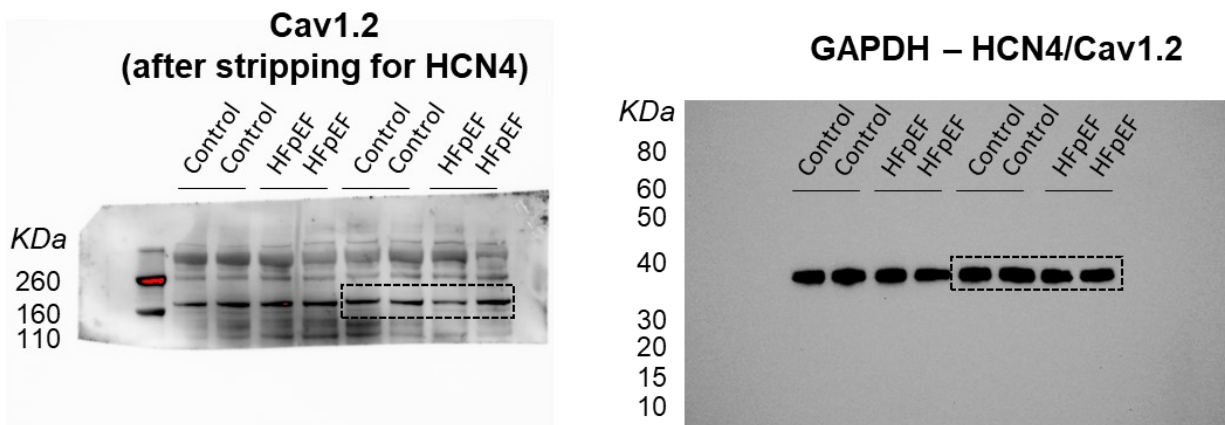
## Full unedited gel for Supplementary Figure 1B



## Full unedited gel for Supplementary Figure 3A



## Full unedited gel for Supplementary Figure 3C



Online Figure XV. Uncut gel blot.

## Online Tables Legends

**Online Table I. Echocardiographic parameters in Dahl salt-sensitive rats fed with normal salt diet (control) or high salt diet (HFpEF).**

	Control	HFpEF
Heart rate (bpm)	372.2 ± 8.2	348.1 ± 9.2
Ejection Fraction (%)	73.7 ± 0.6	72.7 ± 1.3
Fractional shortening (%)	42.6 ± 1.6	43.1 ± 1.0
Peak mitral E velocity (mm/sec)	934.9 ± 28.6	934.8 ± 41.3
Peak mitral A velocity (mm/sec)	612.9 ± 25.9	718.6 ± 36.1*
E/A ratio	1.55 ± 0.04	1.31 ± 0.02***
Peak MVA E' velocity (mm/sec)	70.7 ± 3.8	49.3 ± 2.0***
E/E' ratio	13.6 ± 0.5	19.1 ± 0.6***
LVAW;d (mm)	1.5 ± 0.05	1.9 ± 0.08***
LVID;d (mm)	7.4 ± 0.2	7.5 ± 0.2
LVPW;d (mm)	1.9 ± 0.04	2.2 ± 0.1***
LVAW;s (mm)	2.8 ± 0.1	3.1 ± 0.1*
LVID;s (mm)	4.2 ± 0.2	4.4 ± 0.2
LVPW;s (mm)	3.1 ± 0.1	3.7 ± 0.1***

Data are expressed as mean ± SEM. n=17. animals in each group. Unpaired Student t test. MVA = mitral valve annulus, LVAW = left ventricular anterior wall thickness (d= diastolic; s= systolic), LVID = left ventricular internal diameter (d= diastolic; s= systolic), LVPW = left ventricular posterior wall thickness (d= diastolic; s= systolic). Unpaired Student *t*-test. \**P* < .05 and \*\*\**P* < .001 vs control.

**Online Table II. Echocardiographic parameters in C57BL6 mice fed with a standard diet (control) or high fat diet plus drinking water containing Nω-nitro-L-arginine methyl ester (2-hit HFpEF).**

	<b>Control</b>	<b>2-hit HFpEF</b>
Heart rate (bpm)	455.9 ± 10.7	472.2 ± 18.8
Ejection Fraction (%)	71.6 ± 2.2	75.6 ± 1.8
Fractional shortening (%)	40.6 ± 1.8	43.8 ± 1.8
Peak mitral E velocity (mm/sec)	556.5 ± 14.0	687.1 ± 29.8 <sup>***</sup>
Peak mitral A velocity (mm/sec)	379.8 ± 19.8	359.7 ± 24.8
E/A ratio	1.5 ± 0.05	1.9 ± 0.07 <sup>***</sup>
Peak MVA E' velocity (mm/sec)	22.7 ± 1.5	14.1 ± 0.7 <sup>***</sup>
E/E' ratio	25.3 ± 1.2	49.6 ± 2.28 <sup>***</sup>
LVAW;d (mm)	0.91 ± 0.03	1.02 ± 0.01 <sup>**</sup>
LVID;d (mm)	3.44 ± 0.1	3.60 ± 0.1
LVPW;d (mm)	0.86 ± 0.03	1.00 ± 0.02 <sup>**</sup>
LVAW;s (mm)	1.28 ± 0.04	1.43 ± 0.05 <sup>*</sup>
LVID;s (mm)	2.54 ± 0.1	2.54 ± 0.1
LVPW;s (mm)	1.08 ± 0.04	1.25 ± 0.05 <sup>*</sup>

Data are expressed as mean ± SEM. n=12. animals in each group. Unpaired Student t test. MVA = mitral valve annulus, LVAW = left ventricular anterior wall thickness (d= diastolic; s= systolic), LVID = left ventricular internal diameter (d= diastolic; s= systolic), LVPW = left ventricular posterior wall thickness (d= diastolic; s= systolic). Unpaired Student *t*-test. \**P* < .05, \*\**P* < .01, and \*\*\**P* < .001 vs control.

**Online Table III. Echocardiographic parameters in Sprague-Dawley rats after 9 weeks of permanent ligation of the left anterior descending coronary artery (HFrEF) or sham procedure (Sham).**

	<b>Sham</b>	<b>HFrEF</b>
Heart rate (bpm)	317 ± 16.1	292 ± 11.9
Ejection Fraction (%)	75.3 ± 1.8	39.2 ± 1.9***
Fractional shortening (%)	46 ± 1.6	20.2 ± 1.1***
Peak mitral E velocity (mm/sec)	820 ± 62.2	828.2 ± 48.7
Peak mitral A velocity (mm/sec)	602.1 ± 95.2	591.9 ± 47.7
E/A ratio	1.4 ± 0.2	1.4 ± 0.1
Peak MVA E' velocity (mm/sec)	59.5 ± 6.3	43.8 ± 2.9
E/E' ratio	14.3 ± 1.7	19.3 ± 1.7
LVAW;d (mm)	1.8 ± 0.1	1.0 ± 0.1***
LVID;d (mm)	8.4 ± 0.2	10.3 ± 0.3**
LVPW;d (mm)	1.9 ± 0.2	1.8 ± 0.1
LVAW;s (mm)	3.0 ± 0.1	1.8 ± 0.2***
LVID;s (mm)	4.9 ± 0.2	7.9 ± 0.3***
LVPW;s (mm)	3.3 ± 0.2	2.4 ± 0.2*

Data are expressed as mean ± SEM. n=5. animals in each group. Unpaired Student t test. MVA = mitral valve annulus, LVAW = left ventricular anterior wall thickness (d= diastolic; s= systolic), LVID = left ventricular internal diameter (d= diastolic; s= systolic), LVPW = left ventricular posterior wall thickness (d= diastolic; s= systolic). Unpaired Student *t*-test. \**P* < .05, \*\**P* < .01, and \*\*\**P* < .001 vs sham.

**Online Table IV. Transcriptional profiling of all coding genes identified in control and HFpEF SAN tissue.**

**Online Table V. Differentially expressed genes associated with HFpEF SAN diseases.** Ingenuity Pathway Analysis identification of enriched upregulated and downregulated canonical pathways.

**Online Table VI. Gene ontology of the significant differentially expressed genes.** Ingenuity Pathway Analysis was used to assign functional classifications of molecular function, biological processes, and cellular components.

**Online Table VII. Collection of HFpEF SAN models (n = 69) with distinct membrane and  $\text{Ca}^{2+}$  clock parameters values that satisfied our constraint.**

**Online Table VIII. Simulated biophysical effects of 1  $\mu\text{M}$  isoproterenol.**

Current	Parameter shifted
$I_f$	shift of $y_\infty$ and $\tau_y$ by 7.5 mV
$I_{\text{NaK}}$	Increase of $I_{\text{NaK,max}}$ by 20%
$I_{\text{CaL}}$	Increase of the maximal conductance by 23%; shift of $dL_\infty$ and $\tau_{\text{dL}}$ by -8 mV; reduction of the slope factor $k_{\text{dL}}$ by 27%
$I_{\text{Ks}}$	Increase of $g_{\text{Ks}}$ by 20%; shift of $n_\infty$ and $\tau_n$ by -14 mV
<b>SERCA pump</b>	Increase of $P_{\text{up}}$ by 25%

$I_f$ : funny current;  $y_\infty$ : steady-state curve of  $I_f$ ;  $\tau_y$ : activation time constant of  $I_f$ ;  $I_{\text{NaK}}$ : sodium/potassium pump current;  $I_{\text{CaL}}$ : L-type  $\text{Ca}^{2+}$  current;  $dL_\infty$ : steady-state activation curve of  $I_{\text{CaL}}$ ;  $\tau_{\text{dL}}$ : activation time constant of  $I_{\text{CaL}}$ ;  $k_{\text{dL}}$ : slope factor of  $I_{\text{CaL}}$ ;  $I_{\text{Ks}}$ : slow delayed rectifier  $\text{K}^+$  current;  $g_{\text{Ks}}$ : conductance of  $I_{\text{Ks}}$  (slow delayed rectifier  $\text{K}^+$  current);  $n_\infty$ : slow delayed rectifier  $\text{K}^+$  current;  $\tau_n$ : activation time constant of  $I_{\text{Ks}}$ ;  $P_{\text{up}}$ : rate constant for  $\text{Ca}^{2+}$  uptake by SERCA pump into the sarcoplasmic reticulum.

**Online Table IX. Resources Table**

Animals				
Species	Vendor or Source	Background Strain	Sex	Persistent ID / URL
Rat	Charles River	Dahl/Salt Sensitive (SS/JrHsdMcwiCrl) Inbred	Male	<a href="https://www.criver.com/products-services/find-model/dahlsalt-sensitive-rat?region=3611">https://www.criver.com/products-services/find-model/dahlsalt-sensitive-rat?region=3611</a>
Rat	Charles River	Sprague Dawley	Male	<a href="https://www.criver.com/products-services/find-model/cd-sd-igs-rat?region=3611">https://www.criver.com/products-services/find-model/cd-sd-igs-rat?region=3611</a>
Mouse	Charles River	C57BL/6	Male	<a href="https://www.criver.com/products-services/find-model/c57bl6-mouse?region=3611">https://www.criver.com/products-services/find-model/c57bl6-mouse?region=3611</a>
Antibodies				

Target antigen	Vendor or Source	Catalog #	Working concentration	Persistent ID / URL
$\beta$ 1-AR	Abcam	ab3442	1:1000	<a href="https://www.abcam.com/beta-1-adrenergic-receptor-antibody-ab3442.html">https://www.abcam.com/beta-1-adrenergic-receptor-antibody-ab3442.html</a>
$\beta$ 2-AR	Abcam	ab182136	1:1000	<a href="https://www.abcam.com/beta-2-adrenergic-receptor-antibody-epr707n-ab182136.html">https://www.abcam.com/beta-2-adrenergic-receptor-antibody-epr707n-ab182136.html</a>
GRK2	Santa Cruz	sc13143	1:900	<a href="https://www.scbt.com/pt/p/grk-2-antibody-c-9">https://www.scbt.com/pt/p/grk-2-antibody-c-9</a>
pGRK2 <sup>Ser670</sup>	Invitrogen	PA5-77851	1:1000	<a href="https://www.thermofisher.com/antibody/product/Phospho-GRK2-Ser670-Antibody-Polyclonal/PA5-77851">https://www.thermofisher.com/antibody/product/Phospho-GRK2-Ser670-Antibody-Polyclonal/PA5-77851</a>
GRK5	Santa Cruz	sc-518005	1:1000	<a href="https://www.scbt.com/pt/p/grk-5-antibody-d-9">https://www.scbt.com/pt/p/grk-5-antibody-d-9</a>
Hcn4	Alomone	APC-052	1:1000	<a href="https://www.alomone.com/p/anti-hcn4-2/APC-052">https://www.alomone.com/p/anti-hcn4-2/APC-052</a>
Ca <sub>v</sub> 1.3	Abcam	ab85491	1:500	<a href="https://www.abcam.com/cav13-antibody-l48a9-ab85491.html">https://www.abcam.com/cav13-antibody-l48a9-ab85491.html</a>
Ca <sub>v</sub> 1.2	Abcam	ab84814	1:1000	<a href="https://www.abcam.com/cacna1c-antibody-l5746-ab84814.html">https://www.abcam.com/cacna1c-antibody-l5746-ab84814.html</a>
GAPDH	Cell signaling	3683S	1:3000	<a href="https://www.cellsignal.com/products/antibody-conjugates/gapdh-14c10-rabbit-mab-hrp-conjugate/3683">https://www.cellsignal.com/products/antibody-conjugates/gapdh-14c10-rabbit-mab-hrp-conjugate/3683</a>
Anti-mouse, HRP-linked Antibody	Cell signaling	7076S	1:5000	<a href="https://www.cellsignal.com/products/secondary-antibodies/anti-mouse-igg-hrp-linked-antibody/7076">https://www.cellsignal.com/products/secondary-antibodies/anti-mouse-igg-hrp-linked-antibody/7076</a>
Anti-mouse, HRP-linked Antibody	Cell signaling	7074S	1:5000	<a href="https://www.cellsignal.com/products/secondary-antibodies/anti-rabbit-igg-hrp-linked-antibody/7074">https://www.cellsignal.com/products/secondary-antibodies/anti-rabbit-igg-hrp-linked-antibody/7074</a>

#### Data & Code Availability

Description	Source / Repository	Persistent ID / URL
Rhythm-1.2	Matlab code	<a href="https://github.com/optocardiography/Rhythm-1.2">https://github.com/optocardiography/Rhythm-1.2</a>
HFpEF SAN model parameters and dynamics	Matlab code	<a href="https://gitlab.com/annie8899/hfpef_san_manuscript">https://gitlab.com/annie8899/hfpef_san_manuscript</a>
RNA-seq	Gene Expression Omnibus	access number: GSE184120 <a href="https://www.ncbi.nlm.nih.gov/geo/query/acc.cgi?acc=GSE184120">https://www.ncbi.nlm.nih.gov/geo/query/acc.cgi?acc=GSE184120</a>

#### Other

Description	Source / Repository	Persistent ID / URL
-------------	---------------------	---------------------

Rodent Diet with 8% NaCl (rat)	Research Diets	Cat# AIN-76A - D05011703i <a href="https://www.researchdiets.com/opensource-diets/custom-diets">https://www.researchdiets.com/opensource-diets/custom-diets</a>
Rodent Diet with 0.4% NaCl (rat)	Research Diets	Cat# AIN-76A - D10001i <a href="https://www.researchdiets.com/en/formulas/D10001i">https://www.researchdiets.com/en/formulas/D10001i</a>
Rodent Hight Fat Diet (mouse)	Research Diets	Cat# D12492i <a href="https://researchdiets.com/formulas/d12492">https://researchdiets.com/formulas/d12492</a>
Rodent control Diet (mouse)	Teklad	Cat# 2916 <a href="https://www.envigo.com/rodent-natural-ingredient-2016-diets">https://www.envigo.com/rodent-natural-ingredient-2016-diets</a>
L-NAME	Sigma-Aldrich	Cat# N5751 <a href="https://www.sigmaaldrich.com/catalog/product/sigma/n5751?lang=en&amp;region=US">https://www.sigmaaldrich.com/catalog/product/sigma/n5751?lang=en&amp;region=US</a>
Adenosine	Sigma-Aldrich	Cat# A9251 <a href="https://www.sigmaaldrich.com/catalog/product/sigma/a9251">https://www.sigmaaldrich.com/catalog/product/sigma/a9251</a>
Amphotericin B	Sigma-Aldrich	Cat# A9251 <a href="https://www.sigmaaldrich.com/US/en/product/sigma/a4888">https://www.sigmaaldrich.com/US/en/product/sigma/a4888</a>
Isoprenaline hydrochloride	Sigma-Aldrich	Cat# I5627 <a href="https://www.sigmaaldrich.com/catalog/product/sigma/i5627">https://www.sigmaaldrich.com/catalog/product/sigma/i5627</a>
Dobutamine hydrochloride	Sigma-Aldrich	Cat# A4888 <a href="https://www.sigmaaldrich.com/US/en/product/SIGMA/D0676">https://www.sigmaaldrich.com/US/en/product/SIGMA/D0676</a>
RH237	Invitrogen	Cat# S1109 <a href="https://www.thermofisher.com/order/catalog/product/S1109">https://www.thermofisher.com/order/catalog/product/S1109</a>
Blebbistatin	Sigma-Aldrich	Cat# B0560 <a href="https://www.sigmaaldrich.com/catalog/product/sigma/b0560?lang=en&amp;region=US">https://www.sigmaaldrich.com/catalog/product/sigma/b0560?lang=en&amp;region=US</a>
RNeasy Plus Universal Mini Kit	Qiagen	Cat# 73404 <a href="https://www.qiagen.com/us/products/diagnostics-and-clinical-research/sample-processing/rneasy-plus-universal-kits/#orderinginformation">https://www.qiagen.com/us/products/diagnostics-and-clinical-research/sample-processing/rneasy-plus-universal-kits/#orderinginformation</a>
High-Capacity RNA-to-cDNA Kit	Applied Biosystems	Cat# 4388950 <a href="https://www.thermofisher.com/order/catalog/product/4388950#/4388950">https://www.thermofisher.com/order/catalog/product/4388950#/4388950</a>
TaqMan (Adrb1)	Life Technologies	Cat# Rn00824536_s1 <a href="https://www.thermofisher.com/taqman-gene-expression/product/Rn00824536_s1?CID=&amp;ICID=&amp;subtype=">https://www.thermofisher.com/taqman-gene-expression/product/Rn00824536_s1?CID=&amp;ICID=&amp;subtype=</a>
TaqMan (Adrb2)	Life Technologies	Cat# Rn00560650_s1 <a href="https://www.thermofisher.com/taqman-gene-expression/product/Rn00560650_s1?CID=&amp;ICID=&amp;subtype=">https://www.thermofisher.com/taqman-gene-expression/product/Rn00560650_s1?CID=&amp;ICID=&amp;subtype=</a>
TaqMan (Ldha)	Life Technologies	Cat# Rn00820751_g1 <a href="https://www.thermofisher.com/taqman-gene-expression/product/Rn00820751_g1?CID=&amp;ICID=&amp;subtype=">https://www.thermofisher.com/taqman-gene-expression/product/Rn00820751_g1?CID=&amp;ICID=&amp;subtype=</a>
Halt™ Protease and Phosphatase Inhibitor	Thermo Scientific	Cat# 78442 <a href="https://www.thermofisher.com/order/catalog/product/78442#/78442">https://www.thermofisher.com/order/catalog/product/78442#/78442</a>

RIPA Lysis and Extraction Buffer	Thermo Scientific	Cat# 89901 <a href="https://www.thermofisher.com/order/catalog/product/89901">https://www.thermofisher.com/order/catalog/product/89901</a>
Collagenase type II	Worthington	Cat# LS004176 <a href="http://www.worthington-biochem.com/cls/cat.html">http://www.worthington-biochem.com/cls/cat.html</a>
Protease type XIV	Sigma-Aldrich	Cat# P5147 <a href="https://www.sigmaaldrich.com/catalog/product/sigma/p5147">https://www.sigmaaldrich.com/catalog/product/sigma/p5147</a>
Liberase TM	Roche	Cat# 05401151001 <a href="https://www.sigmaaldrich.com/catalog/product/roche/libthro">https://www.sigmaaldrich.com/catalog/product/roche/libthro</a>
Masson's trichrome	Sigma-Aldrich	Cat# HT15 <a href="https://www.sigmaaldrich.com/catalog/product/sigma/ht15?lang=en&amp;region=US">https://www.sigmaaldrich.com/catalog/product/sigma/ht15?lang=en&amp;region=US</a>
Cal-520, AM	AAT Bioquest	Cat# 21130 <a href="https://www.aatbio.com/products/cal-520-am">https://www.aatbio.com/products/cal-520-am</a>
Fluo-4, AM	Invitrogen	Cat# F14201 <a href="https://www.thermofisher.com/order/catalog/product/F14201">https://www.thermofisher.com/order/catalog/product/F14201</a>
Pluronic F-127	Invitrogen	Cat# P3000MP <a href="https://www.thermofisher.com/order/catalog/product/P3000MP">https://www.thermofisher.com/order/catalog/product/P3000MP</a>
ECG telemetry device	Data Sciences International	Cat# CTA-F40 (rat) #ETA-F10 (mouse) <a href="https://www.datasci.com/products/implantable-telemetry/small-animal-telemetry">https://www.datasci.com/products/implantable-telemetry/small-animal-telemetry</a>
1.6 French octapolar electrophysiology catheter	Millar Instruments	Cat# EPR-802 <a href="https://www.adinstruments.com/products/electrophysiology-catheters#product-EPR-802">https://www.adinstruments.com/products/electrophysiology-catheters#product-EPR-802</a>
Swift RNA library kit	Swift Biosciences	Cat# R1096 <a href="https://swiftbiosci.com/swift-rna-library-kit/">https://swiftbiosci.com/swift-rna-library-kit/</a>
Lexogen RiboCop Depletion Kit Human/Mouse/Rat v2	Lexogen Inc.	Cat# 144.24 <a href="https://www.lexogen.com/ribocop-rrna-depletion-kit/hmr/">https://www.lexogen.com/ribocop-rrna-depletion-kit/hmr/</a>
Qubit RNA HS kit	ThermoFisher Scientific	Cat# Q32855 <a href="https://www.thermofisher.com/order/catalog/product/Q32855">https://www.thermofisher.com/order/catalog/product/Q32855</a>
RNA 6000 Nano kit	Agilent Technologies	Cat# 5067-1511 <a href="https://www.agilent.com/store/en_US/Prod-5067-1511/5067-1511">https://www.agilent.com/store/en_US/Prod-5067-1511/5067-1511</a>
Qubit 1X dsDNA HS kit	ThermoFisher Scientific	Cat# Q33231 <a href="https://www.thermofisher.com/order/catalog/product/Q33231">https://www.thermofisher.com/order/catalog/product/Q33231</a>
D1000 ScreenTape	Agilent Technologies	Cat# 5067-5582 and 5067-5583 <a href="https://www.agilent.com/store/en_US/Prod-5067-5582/">https://www.agilent.com/store/en_US/Prod-5067-5582/</a> <a href="https://www.agilent.com/store/en_US/Prod-5067-5583/">https://www.agilent.com/store/en_US/Prod-5067-5583/</a>



## Online Video Legends

**Online Video I. Optical mapping video recorded in spontaneously beating SAN/atrial preparation loaded with a voltage dye from a HFpEF mouse.** Note the change in the location of the earliest activation site in two consecutive beats under isoproterenol stimulation (1  $\mu$ M).

**Online Video II. Laser scanning confocal microscopy 2D movie of intracellular  $\text{Ca}^{2+}$  release recorded in the SAN region of the explanted control SAN/atrial preparation at baseline condition.** Note the rhythmic synchronized  $\text{Ca}^{2+}$  release involving all cells in the focal plane. The green fluorescence indicates the release of  $\text{Ca}^{2+}$  in SAN tissue loaded with  $\text{Ca}^{2+}$  indicator Cal-520. Scale bar: 100  $\mu$ m.

**Online Video III. Laser scanning confocal microscopy 2D movie of intracellular  $\text{Ca}^{2+}$  release recorded in the SAN region of the explanted HFpEF SAN/atrial preparation at baseline condition.** Note the presence of intracellular  $\text{Ca}^{2+}$  waves surrounded by rhythmic cells. The green fluorescence indicates the release of  $\text{Ca}^{2+}$  in SAN tissue loaded with  $\text{Ca}^{2+}$  indicator Cal-520. Scale bar: 100  $\mu$ m.

**Online Video IV. Laser scanning confocal microscopy 2D movie of intracellular  $\text{Ca}^{2+}$  release recorded in the SAN region of the explanted HFpEF SAN/atrial preparation upon isoproterenol stimulation.** Note the erratic synchronism of  $\text{Ca}^{2+}$  release and presence of multiple cells with intracellular  $\text{Ca}^{2+}$  waves. The green fluorescence indicates the release of  $\text{Ca}^{2+}$  in SAN tissue loaded with  $\text{Ca}^{2+}$  indicator Cal-520. Scale bar: 100  $\mu$ m.